

STUDIES ON BISPHOSPHONATE ELUTION FROM ORTHOPAEDIC IMPLANTS

by

Jacintha Roberts, Department of Biomedical Engineering, McGill University

May 2008

A thesis submitted to McGill University in partial fulfillment of the requirements of
the degree of Master of Engineering

© Copyright by Jacintha Roberts 2008



Library and
Archives Canada

Published Heritage
Branch

395 Wellington Street
Ottawa ON K1A 0N4
Canada

Bibliothèque et
Archives Canada

Direction du
Patrimoine de l'édition

395, rue Wellington
Ottawa ON K1A 0N4
Canada

Your file *Votre référence*
ISBN: 978-0-494-51473-3
Our file *Notre référence*
ISBN: 978-0-494-51473-3

NOTICE:

The author has granted a non-exclusive license allowing Library and Archives Canada to reproduce, publish, archive, preserve, conserve, communicate to the public by telecommunication or on the Internet, loan, distribute and sell theses worldwide, for commercial or non-commercial purposes, in microform, paper, electronic and/or any other formats.

The author retains copyright ownership and moral rights in this thesis. Neither the thesis nor substantial extracts from it may be printed or otherwise reproduced without the author's permission.

AVIS:

L'auteur a accordé une licence non exclusive permettant à la Bibliothèque et Archives Canada de reproduire, publier, archiver, sauvegarder, conserver, transmettre au public par télécommunication ou par l'Internet, prêter, distribuer et vendre des thèses partout dans le monde, à des fins commerciales ou autres, sur support microforme, papier, électronique et/ou autres formats.

L'auteur conserve la propriété du droit d'auteur et des droits moraux qui protègent cette thèse. Ni la thèse ni des extraits substantiels de celle-ci ne doivent être imprimés ou autrement reproduits sans son autorisation.

In compliance with the Canadian Privacy Act some supporting forms may have been removed from this thesis.

While these forms may be included in the document page count, their removal does not represent any loss of content from the thesis.

Conformément à la loi canadienne sur la protection de la vie privée, quelques formulaires secondaires ont été enlevés de cette thèse.

Bien que ces formulaires aient inclus dans la pagination, il n'y aura aucun contenu manquant.


Canada

ACKNOWLEDGEMENTS

I would like to express my gratitude to my supervisor Dr. J.D. Bobyn for his guidance and support throughout the course of my thesis. Dr. Bobyn has provided continuous direction and inspiration, as well as a vast amount of knowledge in the field of orthopaedics. His confidence in my abilities helped get me through times of self-doubt and adversity, for which I will always be grateful.

Furthermore, this work could not have been completed without the surgical excellence of Dr. M. Tanzer, who was responsible for the implantation and retrieval of all implants and bones in *in vivo* studies. He was also there to act as a sounding board to discuss unresolved questions relating to my experiments and suggesting additional approaches to analyze the data.

I would also like to thank both Jan Krygier and Dorota Karabasz who provided me with great help with my experiments. Jan built the jig for the experiments and helped in any way possible when needed. Dorota was not only a great help in the laboratory with my experiments, but was kind enough to show me new techniques such as how to prepare samples for BSEM and how to take the images with the electron microscope.

Additionally, both Dr. S. A. Hacking and Dr. L. Lim were responsible in preparing the rat bones for imaging and in teaching me how to use new software (Skyscan 1172 and CTan) to prepare both the data and 3D reconstructions in Chapter 5.

Moreover, Dr. O. Mamer was of great help in analyzing elution samples using GC-MS and negative-ion electrospray techniques. Although, ultimately neither of these techniques proved fruitful, Dr. Mamer consistently provided advice on changes to the technique that would aid the analysis, and for this I am grateful.

This thesis could not have been completed without the kind contribution of Novartis Pharma AG, who donated, both the pure ZA and ^{14}C -ZA that was used in this analysis.

Finally, I would like to express my thanks to my parents, and sisters who have shown unwavering support of me at all times and have always been there to listen during the frustrating times. My boyfriend Raf Karakiewicz, has been a fount of love and support, especially in his ability to always listen at the end of a tough day. Additionally, his perseverance towards higher education in the successful completion of his own masters also served to inspire me to continuously strive towards my own goals.

ABSTRACT

In a 6-week rat model it was demonstrated that a small dose of peri-implant zoledronic acid (ZA) increased local bone formation 3-fold compared with controls. Ancillary *in vitro* studies using ^{14}C -labelled ZA implant doses demonstrated biphasic elution profiles for implants coated with hydroxyapatite; complete ZA release occurred within one to three weeks in serum compared with only 60% ZA release after 12 weeks in water. Implants without hydroxyapatite coating showed more burst-type release profiles and full ZA elution within 24 hours of hydration in serum or water. Canine studies at 6 weeks using implants with ^{14}C -labeled ZA showed that the compound remained localized, with the greatest ZA concentration immediately adjacent to the implant. Although there was evidence of skeletal ZA distribution via diffusion into the circulation, the levels were two orders of magnitude less than at the implant site.

RESUME

Une étude de 6 semaines sur des rats a montré qu'une faible dose de péri-implant acide zoledronique (ZA) augmente de 3 fois la formation locale d'os par rapport aux témoins. In vitro, l'utilisation de ZA marqué au ^{14}C a permis d'obtenir des profils d'élution bi-phasiques pour des implants recouverts de hydroxyapatite. Ces profils ont montré un relargage totale de ZA dans le sérum au bout de une à trois semaines alors qu'il n'était que de 60% après 12 semaines dans l'eau. Les implants non-recouverts d'hydroxyapatite avaient des profils plutôt monophasiques ainsi qu'une élution complète de ZA en 24 heures d'hydratation dans le sérum ou dans l'eau. Une étude canine de 6 semaines utilisant des implants avec ZA marqué au ^{14}C a montré que le composé reste très localisé, avec la plus grande concentration de ZA aux abords immédiats de l'implant. Il a également été montré une distribution de ZA au niveau du squelette par l'intermédiaire d'une diffusion dans le système circulatoire mais seulement à des concentrations deux ordres de grandeur moins élevées qu'au niveau de l'implant.

CONTENTS

1.0	INTRODUCTION	1
1.1	METHODS OF IMPLANT FIXATION.....	2
1.2	BISPHOSPHONATES IN THA.....	3
2.0	LITERATURE REVIEW	5
2.1	DEVELOPMENT OF BIOLOGIC FIXATION.....	5
2.2	FACTORS AFFECTING BONE INGROWTH.....	6
2.2.1	<i>Motion</i>	6
2.2.2	<i>Gaps</i>	7
2.2.3	<i>Pore Size</i>	9
2.2.4	<i>Surface roughness (R_a)</i>	10
2.2.5	<i>Other Factors affecting bone growth</i>	11
2.3	BONE GROWTH ENHANCEMENT TECHNIQUES.....	11
2.3.1	<i>Bone graft materials</i>	12
2.3.2	<i>Growth Factors</i>	13
2.3.3	<i>Electrical and Ultrasonic stimulation</i>	15
2.3.4	<i>Bioactive coatings</i>	15
2.4	POROUS TANTALUM.....	19
3.0	BISPHOSPHONATES	22
3.1	MECHANISM OF ACTION.....	24
3.2	BISPHOSPHONATE USE IN BONE GROWTH.....	25
3.3	ZOLEDRONIC ACID (ZA).....	26
3.4	METHODS OF BP DRUG DELIVERY.....	31
3.4.1	<i>Local Delivery</i>	33
3.5	DRUG LOCALIZATION AND DISTRIBUTION.....	36
4.0	PURPOSE OF THESIS	40
5.0	THE EFFECT OF LOCAL BISPHOSPHONATE DELIVERY ON PERI-IMPLANT BONE FORMATION IN A SIMPLE RAT MODEL	41
5.1	PURPOSE.....	41
5.2	MATERIALS AND METHODS.....	41
5.3	RESULTS.....	44
5.4	DISCUSSION.....	48
6.0	USE OF ^{14}C-LABELLED ZOLEDRONIC ACID FOR CHARACTERIZATION OF THE ELUTION PROFILE FROM POROUS IMPLANTS	50
6.1	PURPOSE.....	50
6.2	MATERIALS AND METHODS.....	51
6.2.1	<i>Preparation of Implants</i>	51
6.2.2	<i>Elution in Water</i>	55
6.2.3	<i>Elution in Serum</i>	56
6.2.4	<i>Water Elution Analysis by Liquid Scintillation</i>	57
6.2.5	<i>Serum Elution Analysis by Liquid Scintillation</i>	58
6.2.6	<i>Analysis of additional items</i>	58
6.3	RESULTS.....	59
6.3.1	<i>Elution Profile from Porous Tantalum Implants</i>	59
6.3.2	<i>Elution Profile from Grit Blasted Solid Titanium Implants</i>	64
6.3.3	<i>Analysis of additional items</i>	69
6.4	DISCUSSION.....	69
6.4.1	<i>Elution Profile from Porous Tantalum Implants</i>	69
6.4.2	<i>Elution Profile from Grit Blasted Solid Titanium Implants</i>	73

6.4.3	Analysis of additional samples.....	74
7.0	DISTRIBUTION OF 14C-LABELED BISPHOSPHONATE AFTER LOCAL ELUTION FROM POROUS IMPLANTS	77
7.1	PURPOSE.....	77
7.2	MATERIALS AND METHODS.....	77
7.2.1	Preparation of Tantalum Implants.....	77
7.2.2	Preparation of Harvested Bones for Analysis.....	78
7.2.3	De-fatting and Drying of Bone Segments.....	79
7.2.4	Grinding and Dissolving of Bone Segments.....	80
7.2.5	Analysis of Bone Solution.....	81
7.2.6	Analysis of De-fatting and Drying Solutions.....	82
7.2.7	Analysis of Radioactivity in Harvested Implant.....	83
7.3	RESULTS.....	84
7.3.1	Localization and Distribution of ZA in Site of Implantation and Other Bones 84	
7.3.2	Analysis of De-fatting and Drying Solutions.....	87
7.3.3	Analysis of Radioactivity in Harvested Implant.....	87
7.3.4	Total Estimate of ZA Distribution and Loss.....	88
7.4	DISCUSSION.....	89
7.4.1	Localization and Distribution of ZA in Site of Implantation and Other Bones 89	
8.0	CONCLUSION.....	93
9.0	REFERENCES	94

LIST OF FIGURES

Figure 1.1	Left image illustrates the anatomy of the hip joint. Right image shows location of hip replacement and metallic implant.	1
Figure 2.1	Hydroxyapatite ($\text{Ca}_{10}(\text{PO}_4)_6(\text{OH})_2$)	16
Figure 2.2	Porous Tantalum Implant	20
Figure 3.1	Bisphosphonate	22
Figure 3.2	Zoledronic Acid (1-hydroxy-2-imidazol-1-yl-phosphonoethyl phosphonic acid)	27
Figure 5.1	Nylon implant coated with commercially pure titanium	42
Figure 5.2	Insertion of ZA into intramedullary canal	43
Figure 5.3	Contact radiograph indicating new bone formation around radiolucent implant when zoledronate is used. Arrows illustrate the outline created by new peri-implant bone formation around the implant that received ZA treatment.	45
Figure 5.4	Reconstructed 3D images of segments from ZA-treated (top) and control femora (bottom).	46
Figure 5.5	Reconstructed 3D images of segments from ZA-treated (left) and control femora (right) from the same animal in Figure 5.4. The view of the distal end of femur shows a greater degree of peri-implant bone formation in the ZA-treated femur.	46
Figure 5.6	Reconstructed 3D images of segments from ZA-treated (top) and control femora (bottom) from a different animal. Once again, more bone is observed in the femur with the ZA treatment.	46
Figure 5.7	Percentage bone within 0.2 mm peri-implant annular space for both femora of each rat and mean \pm SD for all 4 rats.	47
Figure 6.1	Porous tantalum metal implants. Top implant is coated with HA, bottom implant is uncoated	51
Figure 6.2	HA-coated (left) and Uncoated (right) Tantalum struts imaged by BSEM (50x magnification)	51
Figure 6.3	C-14 labelled Zoledronic Acid	52

Figure 6.4 Jig for doping implants consisting of two spindles at either end to secure the implant in place. Implant was then manually doped with aqueous ZA solution using a micropipette.	53
Figure 6.5 Grit Blasted (GB) implants. Top implant is HA coated, bottom implant is uncoated. One end of the HA coated implant was used to grip the implant during plasma spray coating, hence it remained uncoated.	54
Figure 6.6. Calibration curve based on known ZA concentrations for use in determining elution profiles.	58
Figure 6.7 Elution profile for ZA from HA coated tantalum implants in water	60
Figure 6.8. Elution profile of ZA from HA-coated TM implants in serum	61
Figure 6.9 Elution profiles of ZA from HA-coated TM implants in water and serum (averaged data)	62
Figure 6.10 Elution profile of ZA from uncoated TM implants in water and serum (averaged data).	63
Figure 6.11 ZA Elution profile from non-HA coated grit blasted titanium implants in water and serum	65
Figure 6.12 ZA Elution profile from HA coated grit blasted titanium implants in serum.	68
Figure 6.13 ZA Elution profile from HA-coated grit blasted titanium implants in water.	69
Figure 6.14 Comparison of elution techniques using either LSC or UV spectroscopy [66]. Both studies were conducted with HA coated porous tantalum metal implants immersed in water.	75
Figure 7.1 Radiograph of harvested femur containing ZA-doped implant at 6-weeks. Illustration depicts location of sections for C-14 analysis	79
Figure 7.2 Ground bone in bone mill	81
Figure 7.3 Nanograms ZA/g dry bone for each of the Left Femurs along the 18 cm bone length (at each 1 cm interval). Values are much higher immediately adjacent to the implant (slices 6-10) and fall off quickly proximal and distal to the implant.	85
Figure 7.4 Lower concentrations of drug are always observed in the diaphysis of each bone.	86

LIST OF TABLES

Table 6.1 Description of Implants by material and immersion solution	55
Table 6.2 Mean % Mass ZA \pm SD eluted from porous HA coated tantalum implants in water over 12 weeks. Each mean and SD was derived from the measurements of 3 different implants.	60
Table 6.3 Average % Mass ZA eluted from porous HA coated tantalum implants in serum over 1 week period.	61
Table 6.4 ZA Elution results from porous tantalum without HA coating.	64
Table 6.5 Elution results in water of ZA from non-HA coated GB solid titanium implants.	65
Table 6.6 Implant 16 immersed in serum. Results for analysis of entire sample, nearly identical to extrapolated values.	67
Table 6.7 Elution results in water of ZA from HA coated GB solid titanium implants	67
Table 7.1 Concentration of ZA (nanograms per g of dry bone), I=section adjacent to the implant.	84
Table 7.2 Total mass of ZA (M_{ZA}) accounted for in bones analyzed, implant, and defatting and drying solutions. Values for Ether-Acetone and Alcohol are the combined values of the mass of ZA in each solution. * M_{ZA} lost in sample preparation, or excreted, or present in other parts of the skeleton.	89

1.0 INTRODUCTION

Total hip arthroplasty (THA) is a surgical procedure that involves the replacement of the articulating surfaces of the hip joint with implants consisting of an acetabular cup and a femoral stem (Figure 1.1). The articulation between the femoral head and the cup is usually metal against polyethylene, although metal-metal and ceramic-ceramic bearings also exist.

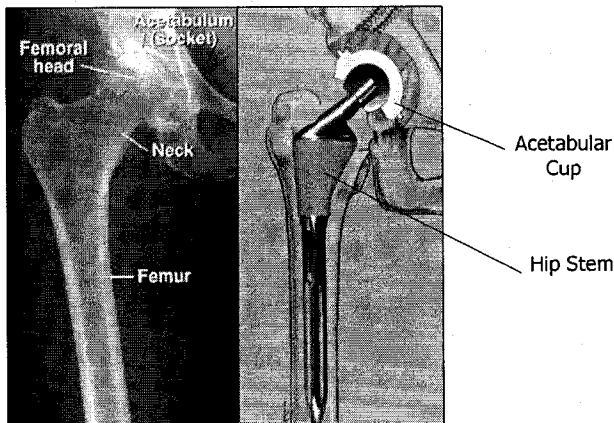


Figure 1.1 Left image illustrates the anatomy of the hip joint. Right image shows location of hip replacement and metallic implant.

Although there exist a variety of reasons for THA (i.e. Paget's disease, arthritis, avascular necrosis or trauma) the most common pathology is arthritis, specifically osteoarthritis (OA). OA is characterized by mechanical wear and tear resulting in loss of cartilage on the surface of articulating surfaces. As cartilage is depleted the boney surfaces of the joint come into contact causing pain for the patient during movement [1].

Thus, the ultimate goal of joint replacement is to eliminate pain while restoring mobility to the patient.

Today, THA is a safe operation with nearly 500,000 procedures performed yearly in the United States alone. The success rate is generally very high, with revision rates in primary cases amounting to only 1-5% percent out to 10 or 20 years after surgery. However, the success of THA is generally inversely proportional to the age of the patient, with aseptic loosening rates often rising in younger patients due to the greater mechanical demands placed on bone-implant interfaces and articulating wear surfaces. The success is also substantially lower in cases of revision, where one or both of the original implants are removed and replaced.

1.1 Methods of Implant Fixation

Two different modalities are employed to mechanically attach implants to the skeleton. One involves the use of bone cement, an acrylic material (polymethyl methacrylate, PMMA) introduced and popularized by Dr. John Charnley in the 1950's. Bone cement is a two-phase material that is mixed together at the operating table and acts as a grouting agent to provide mechanical attachment of the implant to the skeleton. In this method, the cement fills the space between implant and bone in a passive manner to establish fixation. Although strong in compression, PMMA is relatively weak in tension and is quite brittle – it is therefore susceptible to fatigue

failure causing implant loosening, especially in heavier or younger, more active patients that impose higher duty cycles on the material.

An alternative method of fixation involves direct contact between the bone and implant so that bone can form directly on and/or within the implant surface. This modality is referred to as “noncemented arthroplasty” or more commonly, ‘biological fixation’. The success of THA by biological fixation is dependent on the initial stabilization of the implant – ensuring a tight fit between metal and bone. Secure initial stability provides the optimal conditions for secondary fixation by bone ingrowth. Furthermore, biological fixation often involves the use of porous coatings or materials to allow the ingrowth of host bone for purposes of mechanical attachment. This approach depends on initial implant stability as mentioned above, as well as optimum pore size, healthy, vascularized bone capable of healing and regeneration, and a period of postoperative restricted load bearing to maximize the opportunity for bone formation at the implant interface. This approach would further benefit from any process that accelerated the rate and extent of peri-implant bone formation and bone ingrowth [2].

1.2 Bisphosphonates in THA

Bisphosphonates (BPs) are a class of anti-resorptive drugs that cause net bone formation by suppressing osteoclastic activity. This explains their use in bone diseases such as osteoporosis where it is desirable to increase overall bone density and mass. BPs also have potential

application in the biological fixation of total joint arthroplasty implants since they could be used to enhance bone formation at the bone-implant interface. An elegant approach in this regard is to target peri-implant bone through local elution of BP compound directly from an implant – this would avoid unnecessary exposure to other skeletal sites as would occur with systemic delivery. This represents the general topic of research in this thesis.

2.0 LITERATURE REVIEW

2.1 Development of Biologic Fixation

Although considered a relatively common procedure today, it is believed that the first record of a THA was performed in Germany in 1891, with ivory used to replace the femoral head. However, much of the development of work in the field of biologic fixation has been credited to advances in the dental field. As early as 1909 it was recorded that a metallic cage was developed by Greenfield to provide stability for an artificial tooth root. It was not until 1952 that the first macroporous or fenestrated orthopaedic implant (Moore self-locking endoprosthesis) was created. This prosthetic was composed of cobalt-chromium-molybdenum (Co-Cr-Mo) with large empty spaces that allowed mechanical interlock of the implant by healing bone [3]. Further development of porous prosthetic coatings was made in the late 1960's when researchers Hirschhorn and Reynolds fabricated a porous Co-Cr-Mo implant with an average pore size of 10-20 μ m. When implanted into canine cortical bone they observed tissue infiltration of the pores. The first porous pure titanium fibre implant was produced by *Lueck et al* in 1969 [4]. Further development of this material was completed in 1971 by *Galante et al* through moulding and sintering [5].

Through the 1970's many researchers studied the use of porous Co-Cr-Mo to determine the optimum parameters to ensure the maximum amount

of tissue ingrowth. At this time it was common practice for microspheres to be sintered onto the metallic implant. Mechanical push-out tests were performed in canine cortical bone to determine the effectiveness of both small and large pore sizes [4]. *Hirschhorn et al* fabricated titanium implants with pore sizes ranging from 15-200 μ m. Fibrous tissue was observed with the smaller pores (15 μ m), while infiltration of the pores with bone occurred with the larger pore sizes [6]. Although, porous coatings were shown to be advantageous for enhancing bone ingrowth, it was discovered that when porous coatings were applied to titanium implants by sintering or diffusion bonding, the fatigue properties of the material was reduced by about half. In 1970, *Hahn et al* developed plasma sprayed titanium coatings for use in orthopaedic implants. This new technique allowed titanium implants to suffer only a 10% loss of fatigue properties, enabling both the strength of the implant and its biologic fixation [7].

2.2 Factors affecting bone ingrowth

There are a number of factors that can affect the rate and extent of bone growth into a porous implant. The most important factors (motion, gaps and pore size) are described in further detail below.

2.2.1 Motion

Initial stability of the implant is integral to ensuring bony attachment of an implant. Research has shown that excessive motion can inhibit bone

ingrowth, resulting in fibrous tissue infiltration. Fibrous tissue fixation presents a problem; since it is not as rigid as bone, it is like a 'non-union' of a fracture and hence has a greater tendency to be painful for the patient [8]. Studies in animals have provided an indication of the limit of interface micromotion that can be tolerated for bone or fibrous tissue ingrowth. *Burke et al* showed that micromotions of about 40 μ m permitted the formation of bone within a porous titanium surface, however, this was a mixture of woven bone and fibrous tissue. When the micromotion was increased to 75 μ m only fibrous tissue growth was observed [4]. Generally speaking, it is believed that initial implant stability should be such that the interface motion is limited to less than about 50 μ m if bone ingrowth is to reproducibly occur.

2.2.2 Gaps

There exists an upper limit to the distance between the bone and the porous implant for bone ingrowth to still occur. *Kienapfel et al* demonstrated in both loaded and unloaded models the level of bone growth and strength of fixation was limited in the presence of gaps. In a non-weight bearing sheep model, animals received a HA coated porous titanium implant with a 2mm gap, with the contralateral femur containing a press-fit control. After a time interval of 3 weeks it was demonstrated that bone ingrowth was 6-fold higher in the controls as compared to the gap model [4].

Bobyn et al conducted a non-weight bearing canine study to evaluate bone growth into porous coated femoral rods. Rods were prepared to have outside diameters of 5.5, 4.5, 3.2 and 2.5 mm yielding gaps ranging from 0 to 4 mm, with study periods of 4, 8, 12 and 16 weeks. Histological study showed the presence of thin 'spongy' bone around all implants, particularly those with a gap distance of less than 2mm by the 12 week interval. Thicker bone was observed closer to areas of endosteal cortical bone. It was observed that the amount of bone formation increased with decreasing gap size [9].

Dalton et al studied a non-weight bearing canine gap model. In this study 15 canines were bilaterally implanted with porous titanium femoral implants, one of which was coated with hydroxyapatite. Implants were inserted so as to create gap distances of 2.0, 1.0, 0.5 and 0.0mm, with sacrifice at 4, 8, 12, 24 and 52 week time intervals. It was observed that an increase in gap size was associated with a corresponding decrease in both bone ingrowth and fixation strength. Press-fit (0mm) implants achieved an average 43.8% bone ingrowth at 52 weeks, as compared to only 23.4%, 17.1% and 11.1% bone ingrowth at the same time interval for the 0.5mm, 1.0mm and 2.0mm gaps, respectively. Histological examination of the gap filling indicated greater attachment strength in trabecular bone compared with cortical bone, particularly for hydroxyapatite coated implants. All hydroxyapatite coated implants

resulted in increased attachment strength and bone ingrowth at all time intervals. In summary, while direct implant-bone contact is preferable, bone has the ability to bridge gaps of not more than 2mm. Also, the addition of an osteoconductive material such as hydroxyapatite (HA) can increase the potential for ingrowth, particularly with small gaps [10].

2.2.3 Pore Size

There are many different types of porous or textured coatings used for bone ingrowth fixation of implants. Porous coatings are often made by sintered beads or fibre wires to the solid substrate. Textured surfaces can be manufactured by direct casting or by high temperature plasma spray techniques. As long as the material is biocompatible and the implant is sufficiently stable, bone will form (heal) within or onto a wide variety of surfaces.

Bobyn et al conducted a canine study to determine the optimum pore size for bone ingrowth. Implants were formed from Co-Cr-Mo and coated with a cobalt based alloy powder in four particle size ranges to yield implants with pore sizes of 20-50 μ m, 50-200 μ m, 200-400 μ m and 400-800 μ m and a porosity of 30-35%. Canine femora were implanted with one implant of each pore size for periods of 4, 8 and 12 weeks. Pore sizes within 50-400 μ m resulted in the fastest rate of development of fixation strength, the maximum strength being reached by 8 weeks [11].

In a canine acetabular model, it was reported that more bone ingrowth was observed with implants having 450 μ m and 200 μ m pores compared with implants having 140 μ m pores [4]. From these and other studies, it appears that the optimal pore size range is about 100-500 μ m; most commercially available implants are within this range.

2.2.4 Surface roughness (R_a)

The topographical features of an implant surface have also been shown to affect bone formation. Surface roughness is often defined by the parameter R_a which is a measure of the average departure from the center line between the surface peaks and valleys. Surface textures with R_a values of about 2 μ m to 7 μ m have been shown to stimulate osteogenesis, presumably through some sort of interaction with the osteoblast cell membrane. Fine surface textures are most commonly created by grit blasting an implant with glass or alumina particles. Titanium alloy is best suited for this process due to its relative softness compared with cobalt chromium alloy. Another technique, more commonly used in the dental implant industry, is to acid etch the titanium surface to create a slight microtexture. The materials used to fabricate porous coatings, beads or fibre wires, could also benefit from the acid etching process as a means of enhancing the overall bone ingrowth response [12, 13].

2.2.5 Other Factors affecting bone growth

Additional patient-related factors can affect bone ingrowth, these include age, osteoporosis, smoking, surgical technique and drugs. The natural aging process results in a reduction of mesenchymal stem cells, this yields a decrease in the formation of osteoblast progenitors and hence a decline in bone formation. Osteoporosis causes a decrease in both the thickness and number of trabeculae as well as an increase in intracortical porosity - this leads to bone with compromised mechanical properties. Nicotine absorbed through smoking has been demonstrated to interfere with fracture healing by inhibiting vascularization. Drugs used for chemotherapy, corticosteroids and NSAIDs have demonstrated deleterious effects on bone formation. Certain drugs such as bisphosphonates have been shown to be advantageous for altering the bone remodelling cycle in favour of net bone formation; these will be discussed later in more depth [14].

2.3 Bone Growth Enhancement Techniques

Over the years several different approaches have been studied as a means of enhancing the rate and extent of biologic fixation of joint arthroplasty implants. These include the use of bone graft materials, growth factors, electrical stimulation and bisphosphonates, each of which will be briefly discussed in further detail below.

2.3.1 Bone graft materials

Bone grafts are employed to promote bone formation and provide structural support. Grafts may originate from the patient itself (autograft), from a donor (allograft), or may be derived from various bone graft substitutes (e.g. hydroxyapatite, demineralised bone matrix, or composite grafts), with varying results described in the literature. *Kienapfel et al* used cancellous bone autografts and freeze-dried allograft for enhancing bone ingrowth into porous implants. No significant difference was seen between controls and implants with respect to bone ingrowth [15]. *Tagil* studied an unloaded and loaded weight-bearing rabbit model in which animals had the cancellous bone of the tibial marrow cavity replaced with morselized and impacted bone graft prior to insertion of a tibial prosthesis. Increased graft resorption and remodelling was observed in the loaded animals [16].

Pietrzak et al found that the use of demineralised bone matrix (DBM) graft produced some success in revision surgery to bridge a 2-3mm gap. However, DBM grafts suffer from a wide variability in the osteoinductive potential, as natural variances are observed from donor to donor. Furthermore, assessing the effectiveness of the graft in the clinical setting has proven difficult and may be unreliable [17].

The only material to consistently provide useful clinical results is hydroxyapatite. For example, *Sudo et al* found that satisfactory results

were achieved when hydroxyapatite granules were used to pack the acetabular cavity in a cementless THA [18].

2.3.2 Growth Factors

Growth factors are naturally occurring signaling molecules responsible for stimulating cell proliferation and differentiation and include the transforming growth factor β (TGF- β) superfamily. TGF- β is a multi-functional cytokine that is linked to the regulation of growth of a variety of cells, including bone cells. *Aufdemorte et al* studied the effects of recombinant human TGF- β 1 (rhTGF- β 1) on bone healing using titanium implants inserted into the tibia of baboons. The implants allowed for the collection of a native bone sample that was removed at 41 days. A gelatine capsule containing either 1 μ g or 10 μ g of rhTGF- β 1 was applied to the removed bone samples and re-implanted in the tibia; contralateral controls were left untreated. After an additional 22 days of healing, the implants were removed for histological analysis. No significant differences were observed between both TGF- β doses, however increased trabecular bone volumes were seen compared with controls [19].

Bone morphogenetic proteins (BMPs) are growth factors included in the TGF- β superfamily that were first cloned by *Wozney et al* in 1988. They are a set of bone-derived growth factors that aid in the formation of both cartilage and bone [20]. BMPs have been investigated as osteoinductive

agents and are the only growth factors with a known ability to stimulate differentiation of mesenchymal stem cells into chondrocyte or osteoblast progenitors. BMP2 and BMP9 have been identified as osteogenic regulatory molecules. *Kang et al* conducted a study involving the implantation of a titanium implant that was packed with bone graft and recombinant human BMP (rhBMP). Implants were inserted bilaterally into the femoral head of 18 canines after a femoral defect representing avascular necrosis had been created and divided into three groups receiving, (i) Ti implant, rhBMP and bone graft, (ii) rhBMP and bone graft and (iii) bone graft only. After a time interval of 12 weeks the most significant bone response was present in the groups receiving rhBMP. Only minimal defect healing occurred in the implants receiving the bone graft alone [21].

Lind et al has stated that although TGF β , BMP-2 and BMP-7 have been shown experimentally to induce sufficient bone formation for both spinal fusions at the level of bone autografts in sheep, rabbits, and baboons, the clinical effectiveness has yet to be determined in controlled or clinical studies. Furthermore, some growth factors do not provide beneficial effects when administered systemically, due to an insufficient concentration of the factors in the local bone microenvironment. Additionally, some research has shown growth factors to produce toxic side effects and possible neoplasia. Moreover, the manufacture of growth

factors is prohibitively expensive, effectively preventing the routine use of these compounds in the clinical setting [14, 22].

2.3.3 *Electrical and Ultrasonic stimulation*

Electrical stimulation has also been investigated as a method to enhance bone formation. It has been suggested that stimulation of bone matrix proteins and ion flux can be generated during mechanical deformation. In a cascade of events this leads to an increase in metabolic activity. However, with the exception of direct electrical stimulation, no significant results have been achieved with respect to bone ingrowth. Furthermore, this technique is less clinically relevant as results achieved have not provided the level of growth available with other techniques [4]. *Tanzer et al* have demonstrated that low intensity ultrasound can stimulate bone growth in a canine model providing the intensity and duration of treatment are optimized [23]. This modality is somewhat cumbersome however, and has yet to reach clinical application.

2.3.4 *Bioactive coatings*

Bioactive coatings are manmade analogs of the inorganic calcium phosphate phase of bone (Figure 2.1). Hydroxyapatite (HA) and tricalcium phosphate (TCP) are common calcium phosphate coatings that have been shown to increase bone ingrowth or ongrowth at a faster rate over uncoated implants, with widespread use in the field of orthopaedics since

the mid-1980's. HA has also been used clinically for the filling of bone defects or gaps between implant and bone [24].

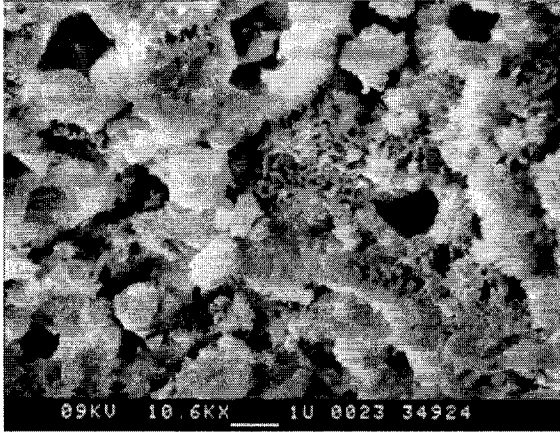


Figure 2.1 Hydroxyapatite ($Ca_{10}(PO_4)_6(OH)_2$)

By increasing the rate and extent of peri-implant bone formation, HA enables a stronger interface resulting in increased implant stability. The mechanism of action whereby HA increases peri-implant bone formation is thought to partially result from the release of both calcium and phosphate ions into the extracellular space. Due to the electronegative potential between the coating and this space an amorphous calcium carbonate layer forms on the outermost layer of the implant. This leads to a cascade of physiological events that leads to an increase in bone formation within and around the implant [24, 25].

In addition to chemical effects, research has demonstrated that HA is inherently microtextured, with a surface roughness of between 3 to 8 μ m when applied by plasma spray techniques. It is this unique surface

topography that is the major contributing factor to the osteoconductive effects observed with HA coatings. *Hacking et al* conducted an *in vivo* canine study to evaluate the contribution of both the surface topography and chemistry of HA. In this study experimental animals received an HA coated titanium femoral implant in the intramedullary canal ($R_a=5.58\pm 1.08\mu\text{m}$) and the contralateral femur received an HA coated titanium femoral implant with a thin (100nm) titanium mask ($R_a=5.58\pm 1.10\mu\text{m}$) to preserve the microtexture, but mask the chemical effects of the HA. Control animals were bilaterally implanted with a polished solid titanium implant ($R_a=0.09\pm 0.02\mu\text{m}$) in the intramedullary canal of one femur and a grit-blasted solid titanium implant ($R_a=3.64\pm 0.72\mu\text{m}$) in the contralateral femur. After a time interval of 12 weeks, the femurs were harvested and prepared and analyzed by undecalcified thin section histology. Histological analysis revealed the lowest rate of bone apposition in control animals, with only 3% apposition observed in samples containing polished titanium implants and 23% bone apposition observed with the grit-blasted titanium implants. Experimental animals demonstrated 74% apposition for the HA-coated implants and 59% apposition for the implants with the Ti-masked HA coating. This clearly demonstrated that although HA chemistry contributes to peri-implant bone formation, the surface topography of HA is the major contributing factor [26].

HA is a biocompatible material, with a calcium phosphate ratio of 1.67 that closely resembles natural bone mineral. It maintains both its volume and morphology upon implantation and resorbs very slowly. HA coatings are typically applied as a thin layer (50-70µm) over all or part of an implant, although thinner coatings of about 10 µm have also been shown effective for enhancing the local bone response [25].

Unlike HA coatings, TCP is known to degrade rapidly and non-uniformly, and is thus less well established in the clinical setting [24]. However, some researchers have found application for this compound as a composite with HA (e.g TCP+HA coating). *Tanzer et al* demonstrated the clinical use of a porous cementless femoral implant coated with a HA+TCP composite coating (80% HA, with remaining 20% composed of TCP and other calcium phosphates) in a randomized double-blind clinical trial. Patients received either a calcium phosphate coated stem or an identical uncoated implant. At a 2-5 year follow-up both groups demonstrated bone ingrowth in nearly all patients (99% for HA+TCP, 98% for controls), with no implants requiring revision due to aseptic loosening. However, fewer radiolucencies were observed in patients receiving the HA+TCP stem, suggesting that the calcium phosphate coating acted to enhance overall osseointegration [27].

HA coatings suffer from a few limitations. Firstly, HA is typically applied using a line-of-sight high temperature plasma spray process that allows

only the outermost layer of a porous implant surface to be coated. HA coatings are very process sensitive, requiring strict control over substrate roughness, temperature and cooling rate. They also tend to be very brittle and hence need to be applied as thin coatings to avoid problems with spalling that can occur with excessive strain. Finally, HA crystals are typically formed of large grains, in the micrometer range; this differs from the small nanometer particles of which natural bone mineral is composed. Biomimetic coatings that apply a 10-30 μ m thick layer of super saturated CaP at low temperatures have been created to overcome this problem. These coatings more closely resemble the mineral phase of bone and have demonstrated increased bone apposition when compared with traditionally coated plasma-spray implants [24].

2.4 Porous Tantalum

Porous tantalum (Trabecular Metal™, Zimmer, Warsaw IN) is a metallic biomaterial that is about 80% porous, as opposed to sintered beaded surfaces that have an average porosity of about 40%. The greater porosity of tantalum implants provides more volume for bone to grow into the implant, thus allowing for a stronger bone-implant interface and faster rate of development of interface strength. Porous tantalum also has desirable mechanical properties, as it is substantially less stiff than other metallic implant materials with a bulk elastic modulus of about 3GPa, similar to

cancellous bone. This results in less stress shielding due to a more even load distribution [28].

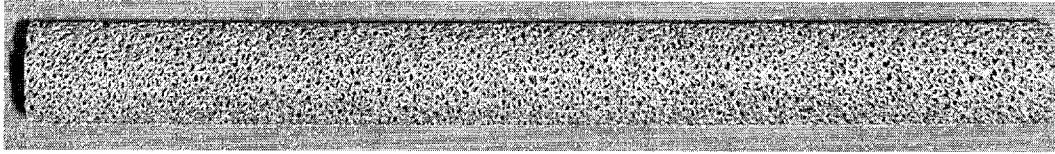


Figure 2.2 Porous Tantalum Implant

Trabecular metal is formed in a unique manufacturing method whereby a pre-form is created with a polyurethane foam that is pyrolysed to create a low density vitreous carbon skeleton with continuous dodecahedron-shaped interconnecting pores. Commercially pure tantalum metal is deposited onto the pre-form by chemical vapour deposition to create the required implant shape [29]. This process results in implants with an average pore size of about $450\mu\text{m}$ with struts that have a surface roughness of $1\text{-}2\mu\text{m}$, yielding a material that is both osteoconductive and suitable for bone ingrowth. Furthermore, the high interconnectivity of the struts results in a high strength-to-weight ratio, and can easily be formed into a variety of shapes. *Bobyn et al* noted 52.9% bone ingrowth at 4 weeks when porous tantalum was implanted into canine femora, increasing to 79.7% at 52 weeks. Push out tests indicated that the shear strength of bone-implant interface was greater than with sintered, beaded, porous implants at equivalent time periods. Furthermore, high fixation strength developed much earlier with porous tantalum because of the higher volume porosity [13].

Porous tantalum has been utilized successfully in a wide variety of implant designs for use in the hip, knee, shoulder and spine for over ten years [13]. It represents the first of a newer generation of highly porous metallic biomaterials that are being developed for orthopaedic surgery.

3.0 BISPHOSPHONATES

Bisphosphonates (BPs) are a class of chemical compounds that effectively inhibit osteoclastic bone resorption, and thus have therapeutic value in bone resorption disorders. These drugs exert their action by selectively adsorbing to bone mineral in osseous tissues, where they are slowly released during remodelling of the skeleton. BPs are analogs of inorganic pyrophosphate, a compound that is a physiological regulator of calcification and resorption, in which the oxygen in the P-O-P had been replaced by a carbon to yield a P-C-P backbone (see Figure 3.1) [30]. BPs are characterized by their binding affinity to calcium phosphate. Once liberated from bone mineral by remodelling, BPs exert their effects by interfering with the actions of osteoclasts, altering the bone remodelling response in favour of bone formation. As such, this class of drugs offers great potential in the field of orthopaedics - altering the bone remodelling response in favour of enhanced bone formation could be utilized to improve the extent and reliability of implant fixation. Many BPs are clinically available to treat various bone resorption disorders such as Paget's disease, hypercalcemia of malignancy and osteoporosis [31].

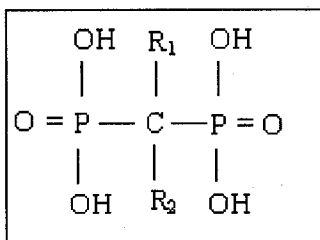


Figure 3.1 Bisphosphonate

The BP structure is identified by the R₁-chain, R₂-chain and two phosphonate groups. The R₁ side chain typically contains a hydroxyl group (R₁=OH) which is required to enhance binding to bone. The presence of a hydroxyl group at the R₁ position increases the affinity for calcium (and thus bone mineral) due to the ability of BPs to bind to calcium ions. The structure and configuration of the R₂ side chain determine the BPs anti-resorptive potency and its binding to HA. In addition to the structure of the R₂ side chain, both phosphonate groups are required for the drugs to ensure the pharmacological activity of the drug. Alterations to one or both phosphonate groups reduce the affinity for bone mineral as BPs covalently bind to HA through exchange of phosphate groups.

BPs can be divided into two main groups: nitrogen containing BPs (N-BPs) and non-nitrogen containing BPs (NN-BPs). Both groups have the basic P-C-P backbone, however, the addition of a nitrogen group in the R₂ side-chain affects both the potency and the BPs mechanism of action. In particular, BPs containing a basic primary nitrogen atom in an alkyl chain have been found to be 10- to 100-fold more potent than 1st generation BPs (NN-BPs). Those containing nitrogen groups within a heterocyclic ring proved to be the most potent, up to 10,000 times more so than first generation BPs [32].

3.1 Mechanism of Action

As previously mentioned, BPs bind strongly to bone mineral, where they are released by osteoclasts during bone resorption. During this process BPs are taken up by osteoclasts where they disrupt the cytoskeleton and cause the disappearance of the ruffled border – the area where the acidic resorption factors are released. Once the ruffled border disappears, osteoclasts are no longer able to resorb bone. It has also been suggested that BPs trigger osteoclast apoptosis causing an increase in bone formation, through the loss of osteoclast function and a reduction in the overall number of osteoclasts. Specifically, N-BPs exert their action by inhibition of the mevalonate pathway – the biosynthetic pathway responsible for the production of sterols (e.g. cholesterol). In particular, N-BPs act on bone metabolism by binding and blocking the enzyme farnesyl pyrophosphate synthase (FPPS). This prevents downstream effects, of intermediates such as farnesyl diphosphate (FPP) and geranyl geranyl diphosphate (GGPP) which are required for protein prenylation of small GTPases (such as Rho, Ras, and Rac). These signalling molecules are involved in the regulation of osteoclast proliferation, survival and cytoskeletal organization, affecting both function and survival of osteoclasts. This aids in restoring the imbalance that may occur in the bone remodelling response, causing an increase in bone formation as osteoclasts are suppressed. However, at this time it is still unknown whether BPs are also able to increase the activity of OBs [33].

3.2 Bisphosphonate Use in Bone Growth

Zou et al demonstrated that chronic administration of alendronate, a N-BP, increased bone formation inside the central canal of a porous tantalum vertebral implant and the region adjacent to the canal, when implanted into pigs. This study suggested that alendronate may stimulate the formation of bone. Furthermore, when administered in low doses, alendronate stimulated the formation of osteoblast precursors. However, no significant histological or radiological differences were observed and no effect was seen on the formation of fibrous tissue at the vertebrae-implant interface [34].

Goto et al studied the amount of mineralized tissue formation that was observed when pamidronate and incadronate were immobilized onto titanium discs. In this *in vitro* study larger osteoblastic cells were observed on titanium discs rather than culture dishes, although more bone-like nodules were observed on calcium coated titanium discs as opposed to pure titanium discs, indicating that BPs stimulated mineralized tissue formation, although at an independent rate to suppression of bone resorption. Furthermore, calcium coated implants containing pamidronate showed an increased number and size of bone-like nodules as compared to incadronate immobilized implants [35].

Bauss et al studied the effects of ibandronate, a N-BP, in an ovariectomized (OVX) monkey model, a model used to represent postmenopausal osteoporotic (PMO) women. Ovariectomy results in estrogen depletion and subsequently causes a decrease in bone mass at the lumbar spine, the femoral neck, head and proximal femur, in addition to increased bone turnover. Animals either received daily or intermittent administration of the drug. A progressive loss of bone mass was observed in control animals, while animals receiving ibandronate maintained bone mass and showed a dose-dependant increase in bone strength, bone mineral density, trabecular bone volume and trabecular number [36].

3.3 Zoledronic Acid (ZA)

Zoledronic acid (ZA) is a 3rd generation BP with a nitrogen atom contained in the heterocyclic ring of the R₂ group, as in illustrated in Figure 3.3 below, which further enhances the potency of the drug. To date, ZA is considered to be one of the most potent bisphosphonates and is up to 10,000 times more potent than 1st generation compounds. This drug is clinically available under the trade name ZometaTM or ReclastTM as an intravenous infusion.

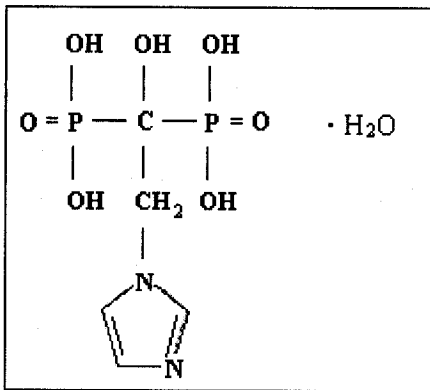


Figure 3.2 Zoledronic Acid (1-hydroxy-2-imidazol-1-yl-phosphonoethyl phosphonic acid)

ZA is indicated for use in the treatment of hypercalcemia of malignancy and Paget's disease and is currently under investigation for the treatment of osteoporosis. Due to its potency, ZA is administered annually and this low-dosing schedule has demonstrated efficacy in ensuring patient compliance to treatment regimens. *Black et al* demonstrated that a single 15-minute infusion of ZA (5mg) has been shown to reduce the number of vertebral, hip and other fractures in osteoporosis patients in a three year study [37]. *Lyles et al* has shown that a single 5mg infusion of ZA within 90 days after hip fracture repair is able to reduce the frequency of new fractures [38].

It is necessary to note that adverse side effects are observed with ZA treatment. Flu-like symptoms have commonly been reported when ZA is administered as an infusion; fatigue, fever, muscle aches and swelling of the lower extremities have also been observed. Although these side effects are relatively minor, more serious effects such as osteonecrosis of

the jaw (ONJ) and renal impairment have been shown to occur in some patients. However, *Higano* reports that annual ZA dosing may be less likely to cause ONJ and renal problems associated with higher doses, resulting in less toxicity, lower costs and enhanced patient compliance [39].

Little et al studied the use of ZA in the treatment of osteonecrosis in a rat model. In this model of traumatic osteonecrosis, initiation of bone repair was observed within the time course of the experiment in all three groups, i) saline operated, ii) ZA given sub-cutaneously two weeks pre-operatively, and iii) ZA treatment given sub-cutaneously at 1 and 4 weeks post operatively. Histological evaluation revealed that saline operated controls had resorbed much of the epiphysis, while treatment groups receiving ZA either pre- or post-operatively resulted in preservation of the femoral head architecture. Furthermore, animals treated with ZA showed improved femoral head shape and significant increase in trabecular number over saline animals, indicating bone repair and new bone formation [40]. *Little et al* further investigated the appropriate dose and schedule required for an increase in bone formation to be observed. This study investigated a rat model of Perthes disease where animals were assigned to one of three groups: i) saline monthly, ii) 3 doses of 0.05mg/kg ZA monthly and iii) 10 doses of 0.015 mg/kg weekly. This dosing schedule resulted in all treatment animals receiving a total ZA dose of 0.15mg/kg over the 15-

week time period. At the end of the time interval a range of femoral deformities from spherical to flat were observed, with radiographs showing increased epiphyseal ossification in ZA treated animals [41].

Bobyn et al investigated the effect of a single dose of ZA on bone ingrowth within a tantalum ulnar implant. Seven dogs received single intravenous dose of ZA (0.1mg/kg) immediately following bilateral implantation of porous tantalum ulnar implants for a time interval of 6 weeks. Histological examination revealed an increase in the size of the bone islands found within the implant; islands were 69% larger than in control animals from a previous study, however, the number of bone islands was nearly the same. Furthermore, 85% more bone ingrowth was observed in experimental animals as compared with controls. These results indicated that the administration of ZA caused a net gain in bone growth into porous tantalum implants [42].

Tagil et al implanted sixteen rats with a bone conduction chamber containing a cancellous bone graft in the proximal tibia. Half of the animals received a bone graft from an animal that had been pre-treated with single subcutaneous dose of 0.7mg of ZA while the remaining control animals received bone graft from an animal that had been administered saline injections. Animals receiving grafts that were pre-treated with ZA showed a 16% increase in the remodeled area, as compared to only 5% in

controls. The graft was almost entirely resorbed in control animals, while BP treated animals demonstrated retention of the graft and the presence of new bone lining the trabeculae of the graft. This study demonstrated an increase in bone density when a graft pre-treated with ZA was implanted [43].

Pampu et al investigated the effect of ZA on bone mineral density (BMD) and bone mineral content (BMC) in a rabbit model at sites of mandibular distraction. Animals underwent distraction osteogenesis of the mandible, after which they were randomized into two groups receiving either an intravenous dose of ZA (0.1mg/kg) or only a saline infusion. After a time interval of 28 days an increase in both BMD (on average 24.7%) and BMC (on average 26%) was seen in experimental animals as compared with controls. Furthermore, ZA caused new bone formation in areas at and around distraction gaps and accelerated the bone healing process after distraction osteogenesis [44].

Bransford et al demonstrated that ZA administration can increase bone mineral content and strength in a rabbit spinal fusion model. In this study 48 rabbits were divided into 3 three groups: i) local ZA treatment with iliac crest bone graft, ii) systemic ZA treatment with iliac crest bone graft, and iii) iliac crest bone only. At a time period of 12 weeks an 86% increase in bone mineral content and 41% increase in spinal fusion mass was seen in

the systemic ZA treatment group, with the local treatment group showing a slightly delayed remodelling response with a 69% increase in BMC and 29% increase in spinal fusion mass. Furthermore, a 31% increase in BMD was observed for both ZA treatment groups, indicating that a single dose of ZA can enhance the rate of spinal fusion [45].

Matos et al studied the effect of ZA on bone remodelling after an osteotomy in a rabbit model. In this study thirty rabbits were divided into two groups where they received either an intraperitoneal infusion of 0.04mg/kg ZA or an equivalent volume of double distilled water. Animals in the experimental group showed an increase in tissue volume and trabecular bone in the metaphysis (prominent site of metabolic turnover), with a decreased amount of fibrous tissue as compared to controls. This demonstrated that ZA is an effective drug to enhance bone formation during fracture healing [46].

3.4 Methods of BP Drug Delivery

In the current clinical setting BPs may be administered orally or intravenously, however, both routes have disadvantages. Oral administration suffers from poor oral absorption of BPs from the gastrointestinal tract; typically only about 1% of the given dose becomes absorbed and available for use. The level of bioavailability is further affected if the drug is taken with certain foods, particularly calcium or iron,

known chelators of BPs. This treatment regimen requires patient compliance, which may be difficult due to the burdensome dosing instructions. Intravenous infusions remove problems with patient compliance, however they are more costly as they must be routinely administered by a health care practitioner. Additionally, intravenous dosing results in an immediate loss of 30-80% of the unmetabolized BP [47, 48]. *Gertz et al* demonstrated that after a 2-hour intravenous infusion of radio-labelled alendronate, plasma concentrations rapidly decreased with only 5% of the initial dose remaining after 6-hours. Furthermore, 50% of the dose was recovered unmetabolized in the urine 72-hours following administration [49]. *Lin et al* demonstrated that after intravenous administration of ^{14}C -alendronate to rats, only 0.36% of the dose was excreted in feces after 24 hours [50]. *Legay et al* conducted a study with [^{125}I]-ZA administered intravenously in rats. Radioactivity of 17-34% of the administered dose was present in rat plasma and urine. When studied in humans 39–46% of the administered dose was recovered 24 hours after infusion, with only trace amounts occurring at later time points [51].

Although satisfactory results have been achieved in studies with systemically delivered BPs, adverse side effects have been reported as mentioned earlier. The oral or intravenous method of delivery is advantageous when it is necessary to alter the remodelling response throughout the entire skeleton, as would be needed for osteoporosis

patients. However, systemic administration is neither necessary, nor ideal, for joint replacement patients, given the need to only affect the bone in the immediate vicinity of the implant. This leads to the topic of this thesis which investigates aspects of immobilizing the bisphosphonate onto an implant by means of an HA coating, for local elution and enhancement of peri-implant bone formation.

3.4.1 Local Delivery

Local delivery of a small amount of a BP from an orthopaedic implant could both avoid deleterious side effects and increase drug bioavailability at the implant site. *Tanzer et al* demonstrated an increase in peri-implant bone formation in a canine model when ZA was delivered locally from an implant. In this study 0.05mg of ZA was immobilized onto porous tantalum implants coated with HA and bilaterally implanted into the ulnar intramedullary canal of four canines. Five control animals received the same tantalum implants without drug coating. Histological analysis and backscattered scanning electron microscopy (BSEM) revealed greater peri-implant bone formation and greater bone ingrowth with the ZA-doped implants. It was hypothesized that this would result in more secure and reliable mechanical implant fixation [52].

Since high doses of systemically administered BPs can have side effects, it is important to understand the dose effect of BPs on bone formation and

implant fixation. *Peter et al* investigated whether ZA could increase the mechanical fixation of a locally eluting implant. Twenty Wister rats were randomized into five groups to receive a HA coated titanium implant in the femoral condyle with 0, 0.2, 2.1, 8.5 or 16µg/implant of ZA. Results indicated that ZA can have a positive effect on bone density and mechanical fixation, though positive results are dose dependant, with higher doses having a negative effect on bone remodelling and biological fixation [53]. In a rat study involving local administration of ^{99m}Tc-pamidronate *Kumar et al* discovered when the BP was directly administered there was an increase in drug uptake at 24 hours, indicating an increased uptake in bone. This study further demonstrated decreased renal uptake and lower urinary excretion of the BP when directly applied as compared to a local intravenous or subcutaneous injection [54].

Many researchers have also compared both systemic and local application of BPs, with greater mechanical fixation observed in the locally delivered group. *Skoglund et al* compared systemic and local delivery of BP to determine which provided greater mechanical fixation of a metallic implant. Stainless steel screws were coated with the N-BP ibandronate and inserted into the proximal tibial epiphysis of seventy-six Sprague-Dawley rats for a period of 14 days. Animals were divided into one of three groups: i) ibandronate injected subcutaneously (systemically), ii) ibandronate locally applied to the insertion hole and iii) controls receiving

subcutaneous saline injection. Biomechanical testing revealed a 30% larger force at failure and a 28% increase in stiffness with animals receiving systemic treatment as compared to controls. The value doubled to 60% larger force at failure when ibandronate was locally applied, with no significant effect on stiffness. This study demonstrated that early fixation is achieved with BPs, with an increase in fixation when the drug is locally applied [55].

Astrand et al conducted studies where alendronate was given either systemically or locally. These rat studies involved inserting a bone chamber containing cancellous bone grafts into the proximal tibial metaphysis. Animals in the systemic study received subcutaneous injections of a high dose of alendronate (205µg/kg/day), a low dose (4µg/kg/day), or saline. The local treatment study involved a similar bone chamber with graft, with either saline or 20µl of 0.1mg/ml of alendronate applied topically. In the systemic study both BP treatment groups showed less bone resorption than controls and a greater increase in bone formation, however, a much higher dose was required to inhibit bone resorption than in the local delivery study. Furthermore, when alendronate was locally applied bone resorption was suppressed after a single application as compared to controls with only $\frac{1}{10}$ of the systemic dose used. By locally delivering the drug only $\frac{1}{10}$ of the dose was required yielding positive results on the local bone microenvironment [56, 57].

3.5 Drug Localization and Distribution

Although local delivery of BPs has demonstrated efficacy in enhancing peri-implant bone formation, it is necessary to know to what extent the drug remains at the site of implantation after application. Various researchers have studied the effects of BP localization and delivery when given systemically. *Monkkonen et al* conducted a rat study involving the intravenous administration of three ^{14}C labelled BPs (etidronate, clodronate and amidronate, all NN-BPs) to determine their *in vivo* distribution. At defined time periods animals were sacrificed and the tissues were analyzed for the presence of radioactivity. This study demonstrated the rapid clearance of BPs from plasma with only low concentrations observed after 12 hours. Autoradiographs indicated a large percentage of the drug was taken up into the skeleton in the vertebrae, ribs, skull and forelimbs. Furthermore, the relative BP concentrations in bone were high at all time points, with peak levels achieved between 30 minutes and 2 hours after drug administration. Over the course of 3 weeks the BP levels were observed to plateau, slowly decreasing with time out to one year. This study indicates that BPs are rapidly cleared from the body when given systemically, although remaining amounts will preferentially accumulate in osseous tissues [58]. When this same group focused on the distribution of clodronate, a NN-BP, similar uptake into bone was observed with the rapid clearance of the drug from other tissues with the exception of the spleen and liver which showed detectable amounts of radioactivity

up until 90 days after administration [59]. The results of these studies were supported in future work by *Gertz et al*, who demonstrated that after a 2-hour intravenous infusion of alendronate, plasma concentrations rapidly decreased with only 5% of the initial dose remaining after 6 hours. Furthermore, 50% of the dose was recovered unmetabolized in the urine 72 hours following administration. Initially radioactivity was present throughout the body, with only 5% of the initial dose present after 1 hour, decreasing to 1% after 24 hours. However, 60-70% of the administered dose was found to accumulate in osseous tissue within 1 hour with high concentrations still present after 71 hours [49].

Furthermore, *Smith et al* demonstrated that ibandronate, a N-BP, is more likely to accumulate in the proximal metaphysis rather than in the distal metaphysis of the bone when given intravenously. This group further observed that a greater amount of BP accumulates in the lumbar vertebrae (L6) as opposed to the tibia. Furthermore, when concentrations from whole bones were compared, higher radioactivities were observed in areas of trabecular bone as there is a higher surface area compared to cortical bone [60]. *Bauss et al* supported this conclusion as his group observed that the mean concentration in the lumbar vertebrae is always about 2 times the concentration found in the tibiae when ibandronate is administered intravenously [61]. However, *Osterman et al* conducted studies that demonstrated that when clodronate is given systemically

(subcutaneously) it localized in the periosteal surface of the femur. The highest amount of activity was seen in the primary spongiosa of the distal femoral metaphysis and in the lower cortical bone of the femoral diaphysis, with high levels seen below the epiphyseal growth plate. Radioactivity in the lumbar vertebrae was about half of that observed in the femur. Autoradiographs depicting the femur in cross-section demonstrated a greater presence of clodronate in the periosteal surface compared with the endosteal surface. Finally, the distribution of ^{14}C -Clodronate throughout different parts of bones or among various bones was uneven depending on the rate of bone turnover [62].

Although, BPs have demonstrated accumulation in bone when administered systemically it is necessary to investigate whether the degree of uptake in tissues outside the target area is decreased when the drug is given locally. *Peter et al* conducted a study involving the local delivery of ZA from within a bone chamber. This study demonstrated that ZA was released rather quickly into the endosteum, within 7 days, where it eventually seems to accumulate in the periosteum over the following 30 days – in contradiction to locally administered BPs. This study suggests that ZA will enter bone through diffusion, but will not diffuse out of the bone afterwards [63].

Little et al demonstrated that when ^{14}C ZA was given locally (as a bolus) at the site of a fracture, the drug was retained at the site in the same order of magnitude as a systemic dose, even though the local dose was $1/10$ the systemic dose. This indicated that a lower amount of the locally applied drug escapes the site of injection, ensuring higher drug bioavailability. However, systemic exposure was still observed with this local delivery method, with the contralateral femur eventually containing half the concentration of ZA observed in the treated femur, presumably through diffusion into the bloodstream via access at the fracture site. In a separate study using a rat fracture model, small quantities of ZA were also observed below the growth plates of both the treated and control femur [64].

There do not appear to be any studies in the literature that measure the skeletal distribution of ZA that elutes locally from an implant. This information would be important to understanding the pharmacokinetics of local drug release and the risk of exposure to ZA at sites remote from the implant.

4.0 PURPOSE OF THESIS

The purpose of this thesis was to investigate several aspects of local delivery of ZA from an orthopaedic implant, when the BP is either locally injected or immobilized onto the device. Specific objectives included the following.

- (i) To study the local bone response to a local injection of ZA in a simple rat model, using femoral intramedullary implants.
- (ii) To study the elution characteristics of ZA from various implant materials, including HA and non-HA coated porous tantalum metal implants and HA and non-HA coated grit blasted titanium implants, when soaked in water and serum.
- (iii) To study the skeletal distribution of ZA, when locally delivered from an eluting implant surgically placed in the femoral intramedullary canal of a canine.

5.0 THE EFFECT OF LOCAL BISPHOSPHONATE DELIVERY ON PERI-IMPLANT BONE FORMATION IN A SIMPLE RAT MODEL

5.1 Purpose

The usual method of examining and quantifying the bone response to orthopaedic implants is with undecalcified thin section histology. While effective and accurate, this method is both time consuming and expensive. Quantification of the peri-implant bone response could also be achieved using micro-CT technology. However, since metallic implants generally interfere with the x-ray signal and confound quantitative measurements and since lab micro-CT equipment enables measurements on only very small bones, the technology is generally not applicable to the usual animal models using larger metallic orthopaedic implants. A possible solution to this problem is to use a smaller animal model and to modify the implant so that it does not interfere with the x-ray signal. The purpose of this study was to quantify the peri-implant bone response to local delivery of a ZA in a simple rat model involving a novel implant design.

5.2 Materials and Methods

Eight nylon implants (20mm long and 1.2mm in diameter) were coated with a thin (100nm) layer of commercially pure titanium (Figure 5.1) using physical vapour deposition, as described by *Hacking et al.* The reason for using a nylon implant was to facilitate the use of microCT for quantifying the peri-implant bone response. Metallic implants generally cause beam

scatter and confound accurate microCT measurements; this problem is avoided with the use of polymer implants. The titanium coating on the implant was added to provide biocompatibility without affecting microCT imaging [65].

A solution of commercially available Zometa™ (Novartis Pharma AG, Basel, Switzerland) in distilled deionized water was diluted to create four 100µl aliquots each containing 10µg of ZA. The aliquots were stored in glass vials in a freezer at -20°C until required. Four aliquots of 100µl distilled deionized water were also prepared.

Four male Sprague Dawley rats each weighing approximately 300g were bilaterally implanted with a nylon implant placed inside the femoral intramedullary canal.

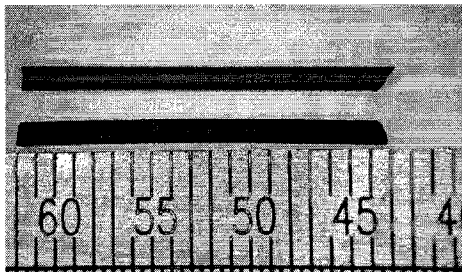


Figure 5.1 Nylon implant coated with commercially pure titanium

On one side a small drill hole was created in the intracondylar notch of the femoral intramedullary canal and 100µl of solution containing 10µg of ZA was slowly injected retrograde (Figure 5.2). This concentration was

chosen to replicate the concentration of drug used in previous studies conducted by *Tanzer et al* in a canine model [52]. An implant was inserted such that it was positioned mostly within the diaphysis and the wound closed with a single resorbable suture. The contralateral side received the same treatment except that 100 μ l of distilled deionized water was injected prior to placing the implant. Injection of the ZA solution resulted in some leakage out of the intramedullary canal prior to implant insertion. It was not possible to quantify the extent of loss hence it was not possible to be certain of the amount of ZA retained within the canal.

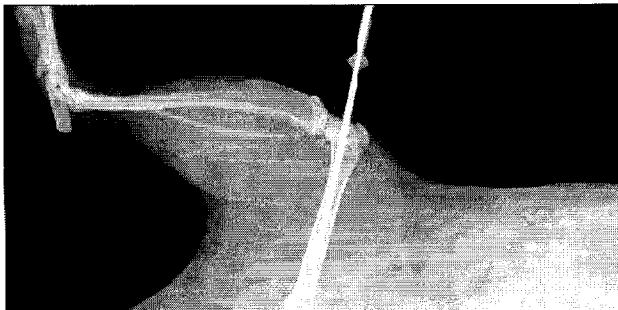


Figure 5.2 Insertion of ZA into intramedullary canal

After six weeks the animals were sacrificed and both femora were harvested. Retrieved femora were cleaned of soft tissue and imaged by contact radiography in a Faxitron MX-20. The bones were subsequently scanned by Micro-CT in a SkyScan 1172 equipped with a 1.3Mp camera (SkyScan, Kontich, Belgium) yielding approximately 2600 vertical slices per femur. Samples were scanned in PBS 1X. Rotation step between each frame was set at 0.45°. X-ray beam was produced with source voltage at 70kV and 100 μ A, and was magnified to 12 μ m/pixel. The

SkyScan produced raw images resembling a radiograph, that had to be reconstructed with NRecon (a software program provided by Skyscan, version 1.4.4.) into 2-dimensional transverse serial cross sections which were used to create the 3D models that used for quantification. These models allowed the visualization of the amount of bone present in the canal around the implants. Quantitative analysis of bone within the canal and within the immediate 0.2mm annular region adjacent to the implant was achieved using SkyScan software CTAn, version 1.7. CTAn allows the user to define and isolate a region of interest (ROI) within the bone that allows for the calculation of the bone volume in that region. The volume of bone in the intramedullary canal approximately 20mm from the growth plate was quantified by applying a grayscale threshold of 88-255. Data were compared between control and ZA-dosed femora using paired student's t tests with $p=0.05$.

5.3 Results

Contact Faxitron radiographs as shown in Figure 5.3 clearly demonstrated the effect of the locally applied drug. The nylon implants themselves were not apparent due to their radiolucency. However, in the ZA-dosed femur from each animal the outline of the implant was visible due to the density of peri-implant bone. In contrast, the implants in the control femora were much less apparent, presumably owing to lesser degrees of peri-implant bone.



Figure 5.3 Contact radiograph indicating new bone formation around radiolucent implant when zoledronate is used. Arrows illustrate the outline created by new peri-implant bone formation around the implant that received ZA treatment.

The greater amount of bone, observed with the contact radiographs, was more readily visualized with the 3D reconstructions of the microCT scans. In Figures 5.4 to 5.6 the implant is not visible, the cortical bone appears as grey, and the intramedullary peri-implant bone appears as yellow. The peri-implant bone on the ZA-dosed side is more abundant and of greater density compared with the control side. This result was consistent among all four animals in the experiment, with a greater degree of peri-implant bone observed in the ZA-dosed femur.

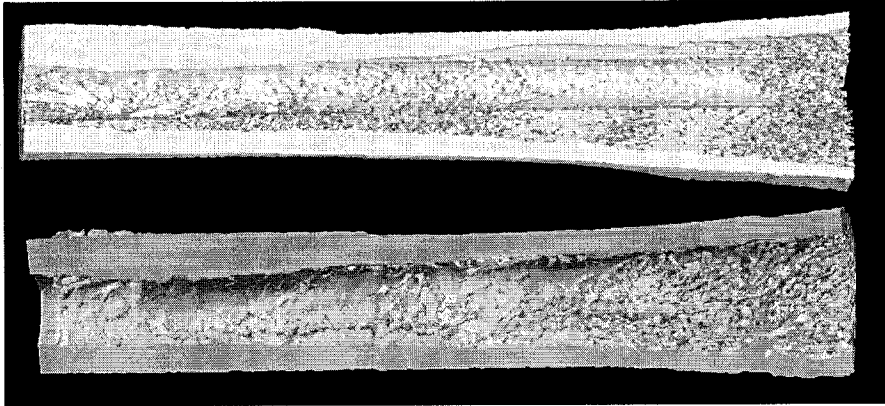


Figure 5.4 Reconstructed 3D images of segments from ZA-treated (top) and control femora (bottom).



Figure 5.5 Reconstructed 3D images of segments from ZA-treated (left) and control femora (right) from the same animal in Figure 5.4. The view of the distal end of femur shows a greater degree of peri-implant bone formation in the ZA-treated femur.

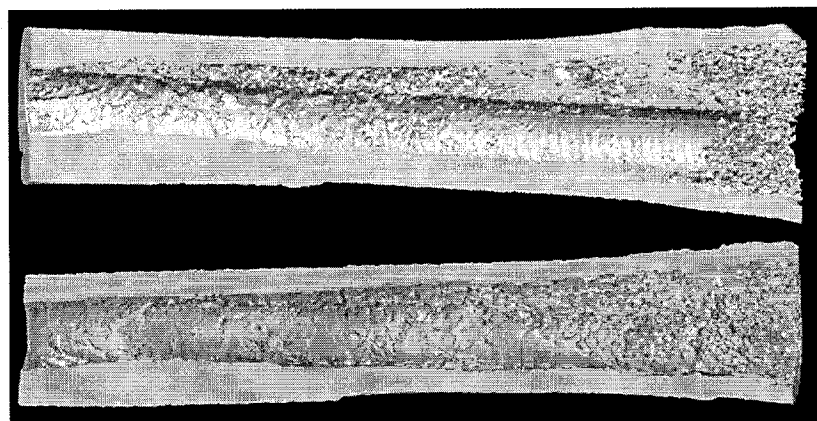


Figure 5.6 Reconstructed 3D images of segments from ZA-treated (top) and control femora (bottom) from a different animal. Once again, more bone is observed in the femur with the ZA treatment.

Quantitative analysis of peri-implant bone revealed that in each animal the volume of peri-implant bone on the ZA-dosed side was greater than on the control side. The mean amount of peri-implant bone for the ZA-dosed femora was 23.6% compared with a mean of 12.6% for the control femora ($p < 0.05$). Quantitative data from reconstructed micro-CT sections are illustrated in Figure 5.7, plotting percentage filling of the peri-implant space in an annular region within 0.2 mm of the implant. In this analysis the mean bone filling of the peri-implant space was 25.3% for the ZA-dosed femora compared with 8.6% for the control femora ($p < 0.05$), about a 3-fold difference.

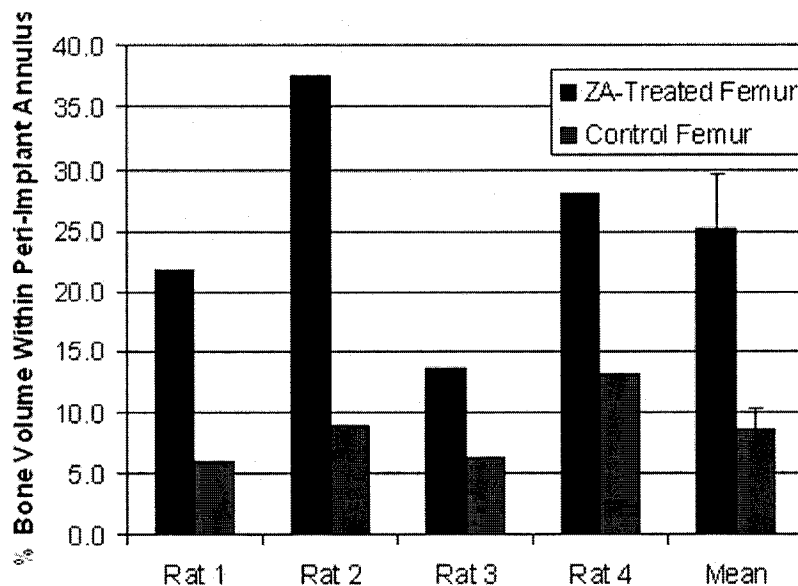


Figure 5.7 Percentage bone within 0.2 mm peri-implant annular space for both femora of each rat and mean \pm SD for all 4 rats.

5.4 Discussion

The method of injecting the ZA at the implant site is not as elegant or controlled as direct elution from an implant. Some loss of drug occurred inevitably due to leaking of the solution prior to implant insertion. It is unknown to what extent ZA might have diffused into the bloodstream and bound to femoral bone on the control side and affected peri-implant bone formation – this issue will be addressed in a subsequent experiment in this thesis. Nevertheless, the effect of ZA delivery on local bone formation was substantial, reproducible, and statistically significant. In this context this experiment served as a valuable proof of concept that corroborated prior studies in the literature showing the value of local ZA delivery for enhancing peri-implant bone formation.

The additional value of this experiment related to the novel animal implant model and the use of titanium coated polymer implants in conjunction with microCT imaging. The model is simple and cost effective and enabled quantitative analysis of peri-implant bone formation through 3D visualization and reconstruction of microCT images. Such analysis on whole bones is not possible with metallic implants or larger animal bones. The described rat model will therefore have further utility in studies of this type. Future work will seek to further analyze the effect of local ZA delivery on the bone microenvironment over additional time points. In such studies it would be preferable to incorporate a method of immobilizing ZA onto the

polymer implant to avoid the imprecision associated with direct injection of
ZA solution within the intramedullary canal.

6.0 USE OF ¹⁴C-LABELLED ZOLEDRONIC ACID FOR CHARACTERIZATION OF THE ELUTION PROFILE FROM POROUS IMPLANTS

6.1 Purpose

The concentration of bisphosphonate eluted from an implant soaked in fluid is a challenge to measure, particularly for 3rd generation compounds like ZA containing a heterocyclic ring. Previous studies analyzing the concentration of eluted ZA from HA coated porous tantalum implants have used chelating agents and ultra-violet visible molecular absorption [66]. This technique and others using mass spectroscopy and negative-ion electrospray have been complicated by the interference of HA phosphate groups with ZA phosphate groups. The result is that detection methods based on phosphate chemistry can yield erroneous results showing ZA elution in greater quantity than was originally deposited on an implant. As such, none of these methods have been able to provide conclusive, reproducible characterization of the ZA release profile from implants. The purpose of this study was to use ¹⁴C-labelled ZA as a means of accurately determining the elution profile of ZA from several types of implants in both water and serum: i) HA-coated porous tantalum implants, ii) non-HA coated porous tantalum implants, iii) HA-coated solid grit blasted titanium implants and iv) non-HA coated solid grit blasted titanium implants.

6.2 Materials and Methods

6.2.1 Preparation of Implants

Tantalum Implants

A total of twelve porous tantalum metal implants 5 mm in diameter and 50 mm in length were manufactured for the elution studies (Figure 6.1). The implants were of two types: as-manufactured porous tantalum and porous tantalum with a thin (10-15 μ m) layer of HA (98% purity, 99% density, 64% crystallinity and a calcium:phosphate ratio of 1.67). The HA coating was applied by a plasma spray line-of-sight technique that resulted in only the outermost tantalum struts coated with HA, leaving the innermost struts uncoated (Figure 6.2).

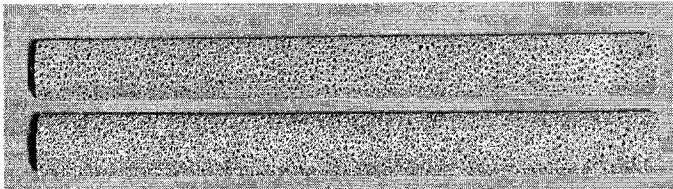


Figure 6.1 Porous tantalum metal implants. Top implant is coated with HA, bottom implant is uncoated

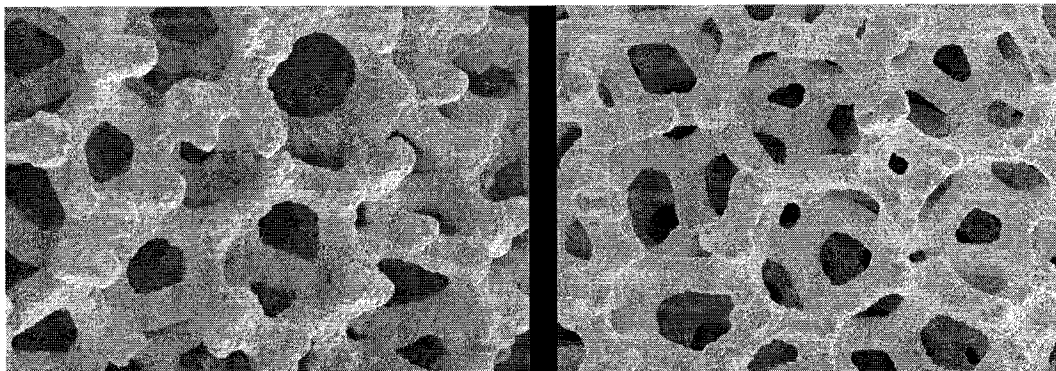


Figure 6.2 HA-coated (left) and Uncoated (right) Tantalum struts imaged by BSEM (50x magnification)

Three HA-coated tantalum implants that were to be immersed in water were doped with a ZA solution prepared from commercially pure ZA (0.04 mg) and ^{14}C -labelled ZA (0.01 mg, specific activity = 6.507MBq/mg, Figure 6.3) that was dissolved together in 500 μl of deionized distilled water (ddH₂O). The total dose of 0.05 mg was the same used in ancillary animal experiments to study the effect on local bone formation [52].

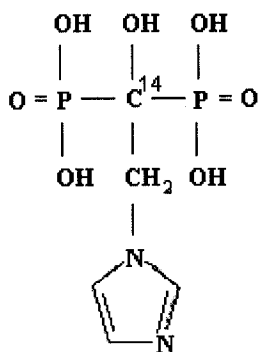


Figure 6.3 C-14 labelled Zoledronic Acid

Implants were weighed with an electronic balance (Denver Instruments Company, model AB-300, Readability 0.1mg) prior to drug impregnation. They were then placed in a spindle jig (Figure 6.4), whereby they could be held at both ends, with one end fixed and the other free to rotate, allowing the surface of the implant to be easily coated. Solution of ZA was slowly distributed drop by drop across the surface of the implant using a micropipette, with 100 μl applied for every $1/5$ rotation of the implant. This technique of ZA deposition took advantage of the known chemical affinity of bisphosphonates for calcium phosphate, the same affinity that enables their selective binding to bone. The ZA was only able to chemically bind

to the outermost HA-coated struts although ZA solution wicked into the interior struts of the implants as well. After each implant was doped the jig was cleaned with 95% alcohol and the jig monitored with a Geiger counter to determine if contamination had occurred. The aqueous ZA solution was prepared from the pure compound (donated by Novartis Pharma AG Switzerland), to prevent any cross reactions that may have arisen from binder, buffers, and fillers that are present in the pharmaceutical formulation. After ZA deposition each implant was placed in an oven to dry at 50°C for 24 hours.

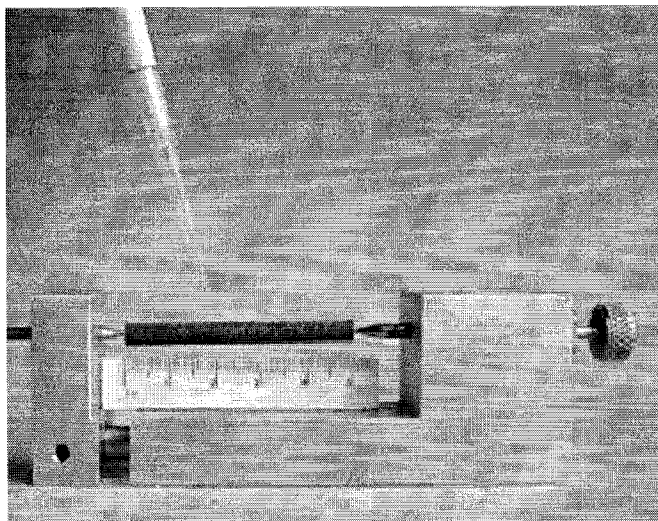


Figure 6.4 Jig for doping implants consisting of two spindles at either end to secure the implant in place. Implant was then manually doped with aqueous ZA solution using a micropipette.

Elution from the remaining nine tantalum implants (3 HA coated and 6 uncoated) of the original twelve implants was analyzed later; these implants were doped with a ZA solution containing a 10-fold lower dose of ^{14}C (^{14}C ZA= 0.1 μg /implant + 0.05mg of ZA). A lower dose was prepared

for these implants in order to conserve the small quantity of radio-labelled drug received from Novartis Pharma.

Solid Grit Blasted Titanium Implants

A total of twelve grit blasted solid titanium implants as seen in Figure 6.5 were used in this study. Six of the implants were coated with a thin HA coating while the remaining six were left untreated. Each implant was coated with a prepared ZA solution containing 0.05mg of cold ZA and 0.1µg of ¹⁴C ZA in a volume of 200µl. A lower volume was used than with the porous tantalum implants since the solid grit blasted implants lacked pores to absorb greater fluid volume. Implants were placed in the jig and coated with 50µl of solution at each ¼ turn. Application of the solution resulted in adhered droplets due to surface tension effects; a small wooden applicator was used to manually disperse the droplets evenly over the surface at each ¼ turn. Once all the solution had been added and the implants were thoroughly dried in an oven at 50°C, they were weighed to ensure that no additional fluid remained.

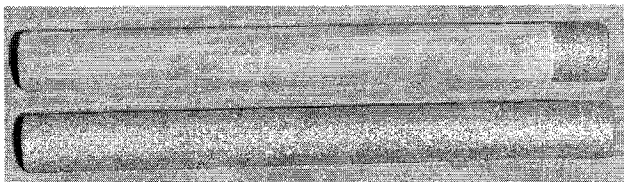


Figure 6.5 Grit Blasted (GB) implants. Top implant is HA coated, bottom implant is uncoated. One end of the HA coated implant was used to grip the implant during plasma spray coating, hence it remained uncoated.

A complete list of the type of implant used and the fluid in which the elution was studied is outlined in Table 6.1.

Implant #	Material	Immersion Solution
1	HA-coated Porous Tantalum	Water
2	HA-coated Porous Tantalum	Water
3	HA-coated Porous Tantalum	Water
4	HA-coated Porous Tantalum	Serum
5	HA-coated Porous Tantalum	Serum
6	HA-coated Porous Tantalum	Serum
7	Uncoated Porous Tantalum	Water
8	Uncoated Porous Tantalum	Water
9	Uncoated Porous Tantalum	Water
10	Uncoated Porous Tantalum	Serum
11	Uncoated Porous Tantalum	Serum
12	Uncoated Porous Tantalum	Serum
13	Uncoated Grit Blasted Titanium	Water
14	Uncoated Grit Blasted Titanium	Water
15	Uncoated Grit Blasted Titanium	Water
16	Uncoated Grit Blasted Titanium	Serum
17	Uncoated Grit Blasted Titanium	Serum
18	Uncoated Grit Blasted Titanium	Serum
19	HA-coated Grit Blasted Titanium	Water
20	HA-coated Grit Blasted Titanium	Water
21	HA-coated Grit Blasted Titanium	Water
22	HA-coated Grit Blasted Titanium	Serum
23	HA-coated Grit Blasted Titanium	Serum
24	HA-coated Grit Blasted Titanium	Serum

Table 6.1 Description of Implants by material and immersion solution

6.2.2 Elution in Water

Three HA-coated, three uncoated tantalum implants, three HA coated grit blasted implants and three uncoated grit blasted implants were placed into individual vials and immersed in 7ml of ddH₂O such that the implants were fully submerged and surrounded by fluid and maintained at 37°C and

vortexed for 5s. Vials were then kept in an oven at 37°C, sealed to prevent fluid evaporation. At pre-defined sampling intervals (5min, 15min, 30min, 1hr, 3hr, 12hr, 24 hr, 1 week, and weekly thereafter) each implant was removed from solution, the solution was vortexed for 5s and a 3.0 ml aliquot was withdrawn for analysis by liquid scintillation counting. Each implant was placed into a clean vial and re-immersed in 7ml of fresh ddH₂O and the process was repeated at each time interval. After each time interval a Geiger counter was employed to monitor the laboratory bench-top, oven, tweezers and any other item that may have come into contact with the radioactive material, and the CPMs recorded. Any contaminated material was suitably cleaned with soap and water and then rinsed in 95% alcohol and measured again with the Geiger counter until only background counts were present.

6.2.3 Elution in Serum

Three HA-coated, three uncoated tantalum implants, three HA coated grit blasted implants and three uncoated grit blasted implants were immersed in 100% bovine calf serum (Hyclone, $\rho=1.031\text{g/ml}$). Serum was prepared with 20ml of EDTA, 3ml Streptomycin and 5 ml Amphotericin to 500ml of serum (to prevent calcium precipitation and bacterial growth), and agitated prior to use. These implants were also maintained at 37°C and handled in the same manner as the implants immersed in water.

6.2.4 Water Elution Analysis by Liquid Scintillation

Water elution samples were vortexed for 1 minute to ensure even drug distribution and then placed in 9 ml (3:1 cocktail to sample volume) of scintillation cocktail (Ultima Gold AB, Perkin-Elmer USA) and read for 3 minutes in a Tri-Carb 2100TR scintillation counter. A calibration curve ($r^2=0.9999$) as shown in Figure 6.6 was generated using standard ZA solutions with the following concentrations: 0, 0.025, 0.05, 0.1, 0.25, 0.5, 1.0, 5.0, 10.0, 30.0, 50.0 and 100.0 μ g in distilled deionized water, and measured with the same scintillation cocktail and counter. The concentration of drug in each sample was determined from the calibration curve. Since the ratio of radiolabelled ZA to unlabelled drug was known (1:5), it was possible to determine the total concentration of eluted drug. The % mass eluted was determined by:

$$\% \text{ Mass Released} = \left(\frac{\text{Sample Concentration}}{\text{Initial Concentration}} \right) \times 100\%$$

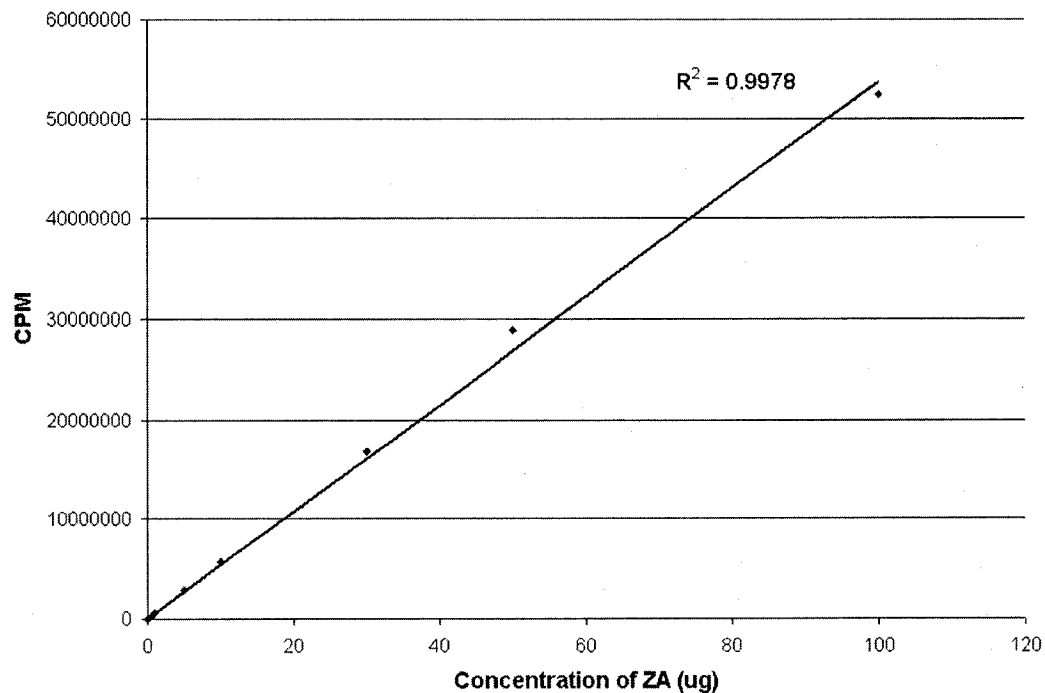


Figure 6.6. Calibration curve based on known ZA concentrations for use in determining elution profiles.

6.2.5 Serum Elution Analysis by Liquid Scintillation

Implants immersed in serum were analyzed in the same manner as the implants immersed in water. However, analysis of serum samples involved a ratio of 10:1 cocktail to sample. Sampling continued at increasing time intervals until only background CPM values were produced during the analysis, indicating the absence of eluted ZA compound.

6.2.6 Analysis of additional items

It was observed that some the HA coated implants immersed in serum yielded % mass elution values slightly over 100%. Geiger countering of the jig spindles used to hold the implants in place while doping, yielded

counts per minute over 1000; however, washing with soap and water and soaking overnight in alcohol failed to remove the drug from the spindles. To determine if the spindles may have been contributing to the abnormally high ^{14}C counts, they were removed from the jig and soaked in 10ml of scintillation cocktail overnight. Additionally, tweezers used to remove implants from tubes were soaked overnight in water and the eluate was analyzed to determine if sample cross-contamination may have occurred. Finally, analysis of a serum sample and a serum sample containing an HA implant was analyzed to determine if the serum was yielding a false positive and thus affecting the values of % mass eluted.

6.3 Results

6.3.1 Elution Profile from Porous Tantalum Implants

The elution data for the 3 HA-coated tantalum implants immersed in water are presented in Table 6.2 and Figure 6.7. The data were very similar between the implants. An average of 34% of the ^{14}C -labeled ZA eluted from the implant within the first 5 minutes. This increased to an average elution of about 50% by 12 hours, with slow but progressive elution up to about 55% of the total out to 12 weeks. After the initial burst release of ZA from the implant, the rate at which the drug was released began to plateau as ~1% of the ZA was released weekly up until week 6. For the remaining time period to 12 weeks the elution rate lowered considerably, with little progression in elution.

Time Interval	% Mass Eluted
0	0.00
5 min	36.54 ± 2.60
15 min	42.10 ± 0.91
30 min	44.91 ± 1.66
1 hr	47.18 ± 0.85
3 hrs	48.72 ± 0.98
12 hrs	50.73 ± 0.95
24 hrs	51.87 ± 0.99
1 wk	52.63 ± 1.04
2 wks	52.88 ± 1.04
3 wks	53.06 ± 1.00
4 wks	53.29 ± 0.79
5 wks	53.67 ± 0.55
6 wks	54.19 ± 0.60
7 wks	54.66 ± 0.84
8 wks	55.20 ± 1.12
9 wks	55.21 ± 1.14
10 wks	55.26 ± 1.14
11 wks	55.33 ± 1.15
12 wks	55.37 ± 1.15

Table 6.2 Mean % Mass ZA ± SD eluted from porous HA coated tantalum implants in water over 12 weeks. Each mean and SD was derived from the measurements of 3 different implants.

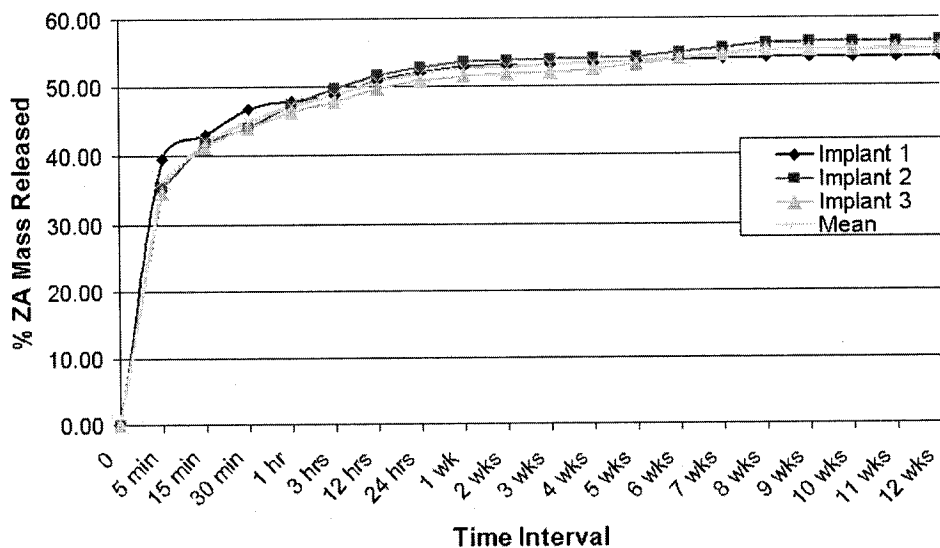


Figure 6.7 Elution profile for ZA from HA coated tantalum implants in water

Although elution in water is a simple first experiment for characterizing the ZA release profile, it was thought to be more realistic to repeat the experiment in serum since the protein content and pH of serum might react differently with the ZA and the HA on the implants. A substantial difference was observed. As with elution in water, good reproducibility (Table 6.3, Figure 6.8) in ZA elution between implants was observed, with low standard deviations.

Time Interval	% Mass Eluted
0	0.00
5 min	68.34 ± 0.23
15 min	83.08 ± 0.70
30 min	88.29 ± 0.95
1 hr	91.36 ± 1.13
3 hrs	93.61 ± 1.01
12 hrs	97.16 ± 1.14
24 hrs	99.82 ± 2.40
1 wk	100.34 ± 2.65

Table 6.3 Average % Mass ZA eluted from porous HA coated tantalum implants in serum over 1 week period.

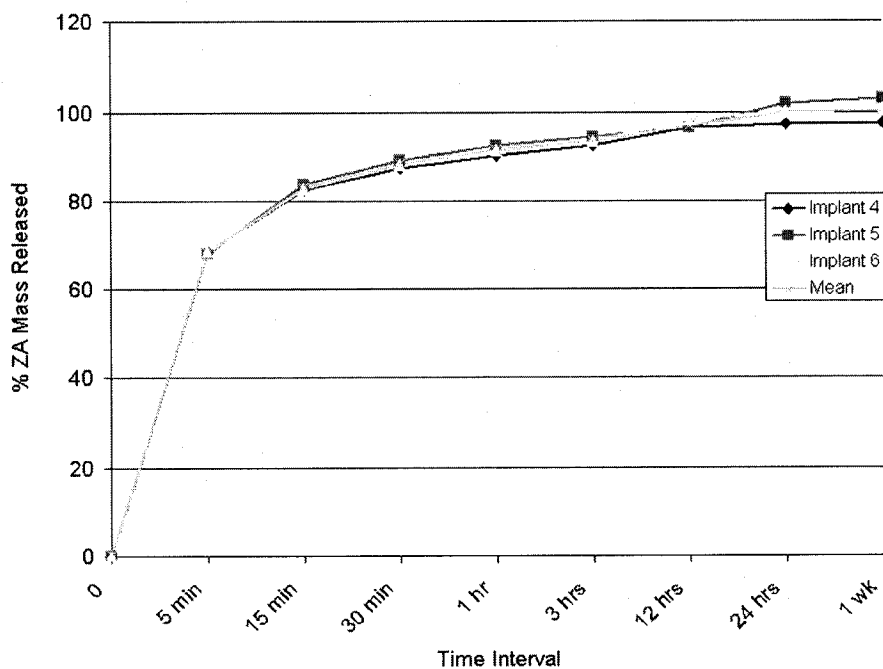


Figure 6.8. Elution profile of ZA from HA-coated TM implants in serum

However, it was observed that during the initial burst release phase approximately double the amount of drug was eluted in the first 5 minutes in serum compared with water, and all the drug was eluted within just one week. A similar biphasic curve was observed in serum as in water; however the rate with which the drug was released into serum was much quicker (Figure 6.9).

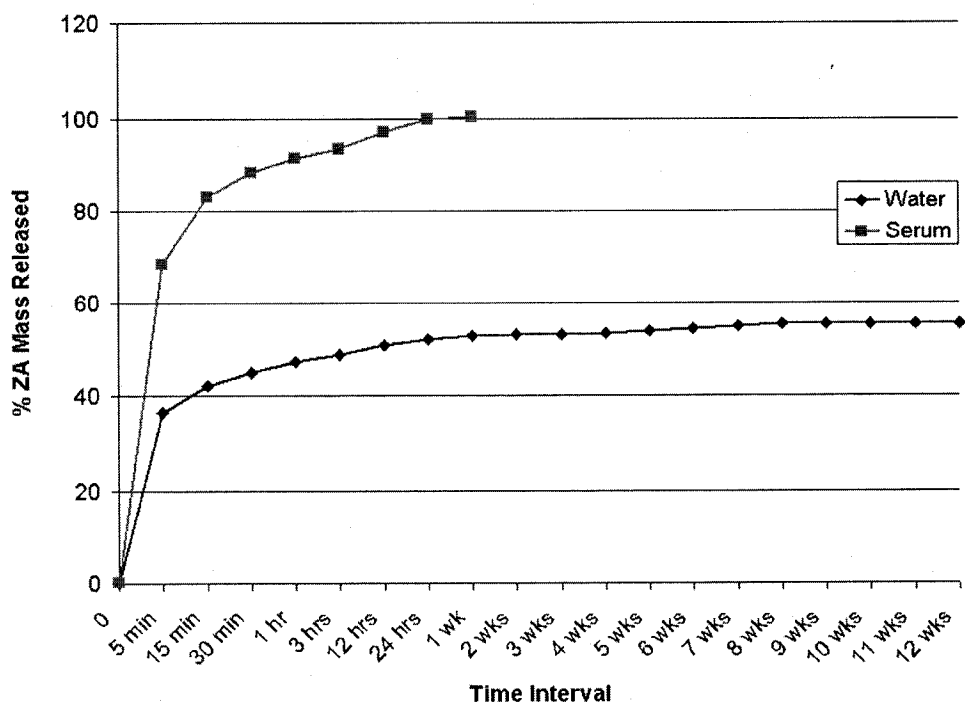


Figure 6.9 Elution profiles of ZA from HA-coated TM implants in water and serum (averaged data)

To further understand the elution profile from porous tantalum implants and the effects of HA coatings, the experiment was repeated with six additional implants that were not HA coated. Three of these implants were immersed in water and three were immersed in serum. As shown in Figure 6.10 and Table 6.4 below, all drug eluted from the implants within the first

12-24 hours, regardless of whether the implant was placed in water or serum.

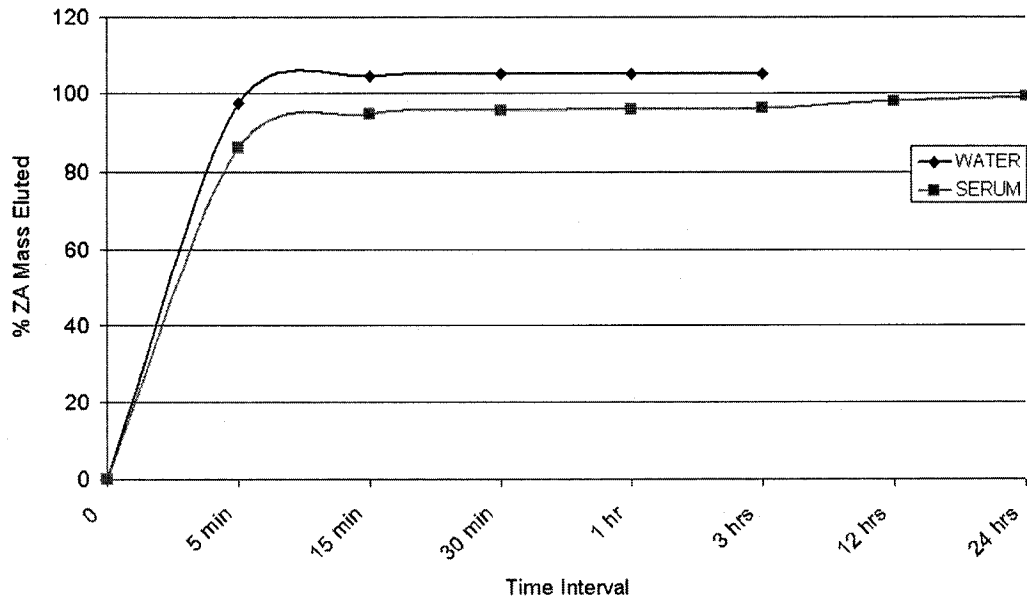


Figure 6.10 Elution profile of ZA from uncoated TM implants in water and serum (averaged data).

However, there was slightly more variation between implants in the serum group. Two of the implants in this group had nearly identical results to each other as well as to the three implants in the “water” group. The third implant in the “serum” group produced slightly lower mass release than the other implants causing it to appear as though uncoated implants had varying results for serum and water.

Time Interval	Water			Avg.	Serum			Avg.
	Implant 7	Implant 8	Implant 9		Implant 10	Implant 11	Implant 12	
0	0.00	0.00	0.00	0.00	0.00	0.00	0.00	0.00
5 min	92.57	102.58	97.50	97.55 ± 5.01	96.45	90.75	71.45	86.21 ± 13.10
15 min	99.69	110.36	103.67	104.57 ± 5.39	105.11	99.70	79.01	94.61 ± 13.77
30 min	100.22	111.03	104.14	105.13 ± 5.47	106.17	100.74	79.75	95.55 ± 13.95
1 hr	100.25	111.13	104.19	105.19 ± 5.51	106.49	100.98	80.01	95.83 ± 13.97
3 hrs	N/A	N/A	N/A	N/A	106.76	101.32	80.23	96.10 ± 14.01
12 hrs	N/A	N/A	N/A	N/A	106.87	101.55	85.27	97.90 ± 11.25
24 hrs	N/A	N/A	N/A	N/A	106.91	104.77	85.50	99.06 ± 11.79

Table 6.4 ZA Elution results from porous tantalum without HA coating.

6.3.2 Elution Profile from Grit Blasted Solid Titanium Implants

In this study, all of the drug eluted from the non-HA coated implants within the first 24 hours, regardless of whether the implants were immersed in water or serum (Figure 6.11), with the exception of one implant (Implant 18) that was immersed in serum.

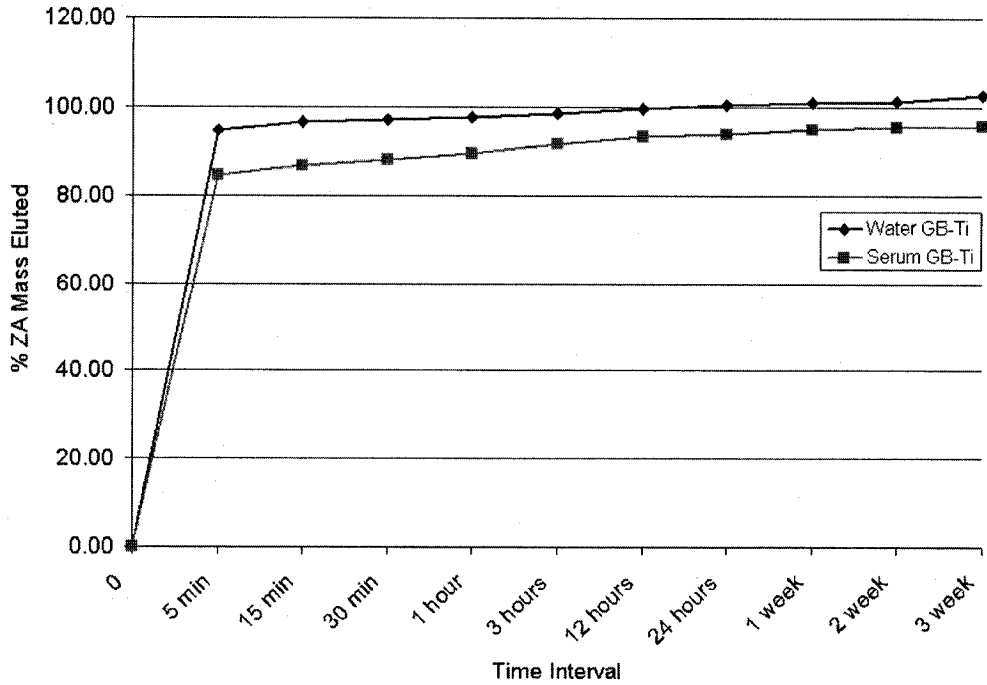


Figure 6.11 ZA Elution profile from non-HA coated grit blasted titanium implants in water and serum

Time Interval	Water			Avg.	Serum			Avg.
	Implant 13	Implant 14	Implant 15		Implant 16	Implant 17	Implant 18	
0	0.00	0.00	0.00	0.00				0.00
5 min	91.11	98.48	94.09	94.56 ± 3.71	96.24	90.21	67.61	84.69 ± 15.09
15 min	93.26	100.34	96.22	96.61 ± 3.56	98.41	92.65	69.54	86.87 ± 15.28
30 min	93.79	100.70	96.78	97.09 ± 3.47	99.42	93.99	70.69	88.03 ± 15.26
1 hr	94.34	101.18	97.31	97.61 ± 3.43	100.87	95.85	72.10	89.61 ± 15.37
3 hrs	95.03	101.95	98.18	98.39 ± 3.46	102.65	98.18	74.08	91.64 ± 15.37
12 hrs	96.07	103.00	99.47	99.51 ± 3.46	104.23	99.91	75.48	93.21 ± 15.50
24 hrs	96.98	103.81	100.25	100.35 ± 3.41	104.99	100.78	76.22	94.00 ± 15.54
1 week	N/A	N/A	N/A	N/A	N/A	N/A	76.90	N/A
2 weeks	N/A	N/A	N/A	N/A	N/A	N/A	77.35	N/A
3 weeks	N/A	N/A	N/A	N/A	N/A	N/A	77.63	N/A

Table 6.5 Elution results in water of ZA from non-HA coated GB solid titanium implants.

Both Implant 18 and Implant 12 yielded lower rates of elution than either of the remaining implants in their respective groups. Furthermore, both of these implants had no HA coating and were immersed in serum. As with the other implants immersed in serum, only 1 ml of the eluate was analyzed by LSC, and from the value of CPMs present in this sample and the known volume of each elution solution, the total CPMs for the sample was extrapolated. For example, if there was 300CPMs in 1.0ml of eluate and the total volume of the eluate sample was 6.0ml, then the total CPMs in the sample was $(300\text{CPMs}) \times (6.0\text{ml})$. This method of extrapolation was considered an accurate method for determining the concentration of ZA elution samples in water that have been well mixed (using a vortex mixer) – ensuring even distribution of the drug in the sample. If the drug were unevenly distributed in the sample, perhaps as a result of inadequate mixing, then a single aliquot might not accurately represent the entire solution. To determine if the drug were unevenly distributed in the serum samples, an implant (Implant 16) was randomly selected and the entire elution sample analyzed in individual 1.0ml aliquots. The total CPMs were added to determine the concentration of ZA (additive method), as opposed to extrapolating from a single aliquot. The values obtained from the additive method were compared with the extrapolation method. This revealed nearly identical results as shown in Table 6.6.

Time Interval	Extrapolated Value	Additive Value	Mean
0	0.00	0.00	0.00
5 min	96.24	95.58	95.91 ± 0.47
15 min	98.41	97.67	98.04 ± 0.52
30 min	99.42	98.66	99.04 ± 0.54
1 hr	100.87	99.96	100.42 ± 0.64
3 hr	102.65	101.75	102.20 ± 0.64
12 hr	104.23	103.24	103.74 ± 0.70
24 hr	104.99	104.04	104.62 ± 0.67

Table 6.6 Implant 16 immersed in serum. Results for analysis of entire sample, nearly identical to extrapolated values.

The HA-coated grit blasted titanium implants showed slower elution rate than those without HA coating. After 5 minutes, a mean of 65.1% ZA eluted from the HA-coated implants in serum (Table 6.7). After a period of 24 hours all the drug from the implants soaked in serum was eluted (Figure 6.12).

Time Interval	Water	Serum
0	0	0
5 min	29.21 ± 2.00	65.13 ± 5.78
15 min	50.01 ± 3.07	79.01 ± 6.64
30 min	61.18 ± 3.51	85.37 ± 6.27
1 hr	68.14 ± 3.86	90.14 ± 6.02
3 hrs	73.19 ± 4.36	93.75 ± 6.05
12 hrs	76.32 ± 4.67	97.31 ± 6.79
24 hrs	78.26 ± 4.78	100.26 ± 8.45
1 week	79.23 ± 4.62	N/A
2 weeks	79.93 ± 4.54	N/A
3 weeks	80.24 ± 4.53	N/A

Table 6.7 Elution results in water of ZA from HA coated GB solid titanium implants

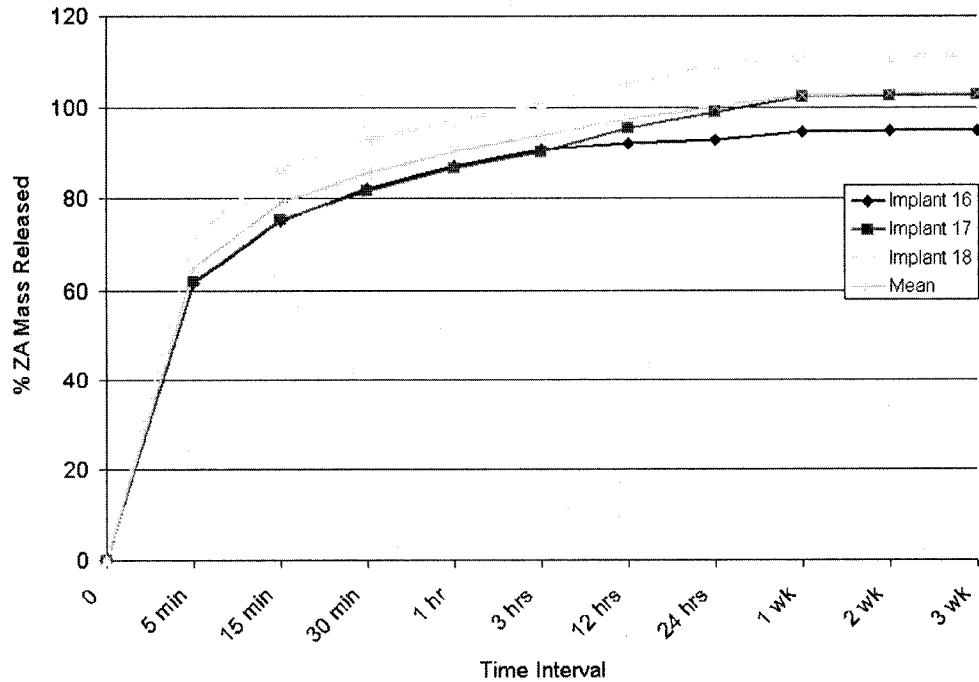


Figure 6.12 ZA Elution profile from HA coated grit blasted titanium implants in serum.

Implants soaked in water showed an initial burst release of the drug up until 1 hour of immersion (Table 6.7, Figure 6.13). After this time, a biphasic elution profile was observed as the remainder of the drug slowly eluted over time, with a mean of 80.2% of the drug released at 3 weeks.

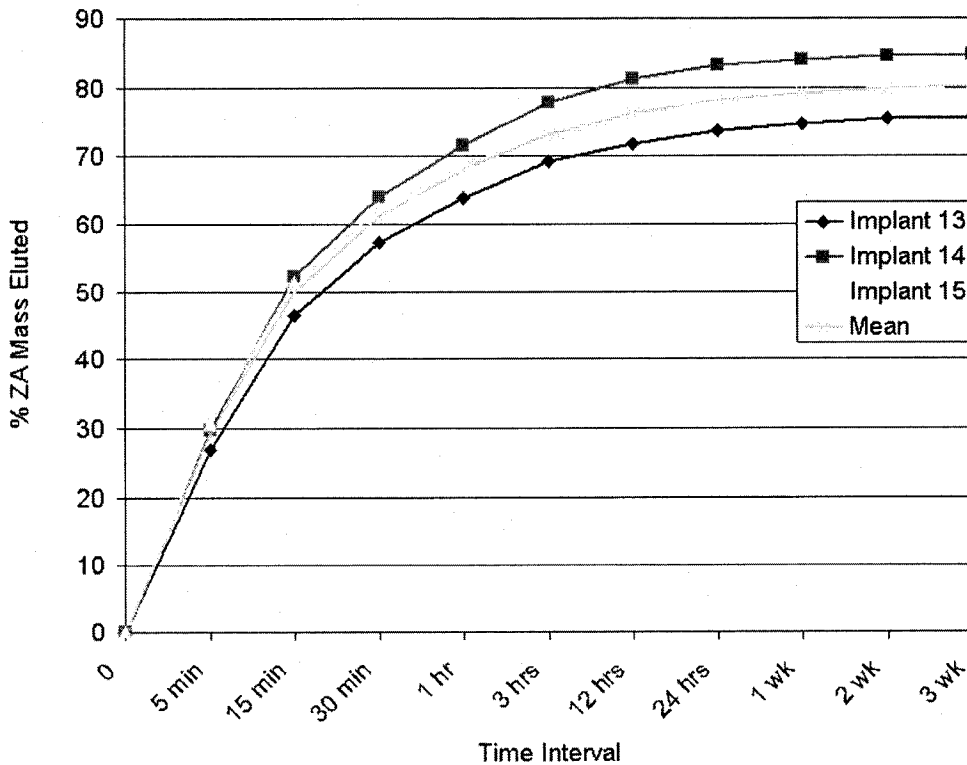


Figure 6.13 ZA Elution profile from HA-coated grit blasted titanium implants in water.

6.3.3 Analysis of additional items

Analysis of the jig spindles by LSC indicated ~1550 CPM or 0.00289 μ g of ZA per spindle; this was equivalent to about 6% of the starting dose for both spindles. Analysis of the tweezers, serum and serum sample with an HA-coated implant revealed values equivalent to background counts.

6.4 Discussion

6.4.1 Elution Profile from Porous Tantalum Implants

The elution profile from HA-coated tantalum implants immersed in water and serum was biphasic in nature, consisting of an early burst release of

ZA in the first 5 to 15 minutes followed by a much slower, progressive release. The early burst is reasonably explained by mere physical attachment of the ZA to the innermost, non HA-coated struts, and easy availability for aqueous dissolution and release. The slower release is explained by dissolution of ZA from the outermost HA-coated implant struts where covalent binding of ZA was possible. The lower rate of elution after the first 6 weeks may be due to resistance of HA dissolution and more tenacious drug attachment after this time. Although, HA-coated tantalum implants immersed in serum produced a biphasic profile, the rate of elution from the implants was much greater than for the same implants immersed in water. Within the first 5 minutes of elution approximately double the amount of ZA was released into the serum sample (mean of 68.34%) than the water samples (mean of 36.54%). The increase in elution rate observed in the serum samples might well have resulted from the use of EDTA, a compound added to reduce the rate of calcium precipitation. EDTA is known to cause an increase in the dissolution of HA, thus releasing the ZA bound to the HA at a much greater rate. Future studies will seek to repeat this elution in the absence of EDTA or using a suitable substitute (e.g. sodium azide) to control the calcium precipitation.

Uncoated tantalum metal implants resulted in the rapid release of ZA within 24 hours, regardless of whether the elution was conducted in water or serum. As previously mentioned, the burst release observed with the

HA-coated implants is attributable to the rapid release of ZA that is only physically bound to the uncoated struts. Without an HA coating, all the ZA is bound by mere physical attachment and thus there is a high rate of drug dissolution. This indicates that the HA coating is instrumental in creating the delayed, biphasic release profile.

In this study several of the non-HA coated implants produced ZA elution values slightly in excess of 100%. However, it is necessary to note that these implants (Implants 4-18) were coated with a 10-fold lower dose of ^{14}C -ZA, which may have contributed to the appearance of % ZA mass released values slightly above 100%. The use of a lower concentration required the inclusion of data points that would have been considered background values in the implants (Implants 1-3) with the higher dose. For example, values for Implants 1-3 ranged from ~100,000CPMs to 800CPMs, with values <200CPMs considered to be background. These values were then multiplied by the appropriate factor, as in the extrapolative method (i.e. 100,000CPMs/3.0ml aliquot yields 600,000CPMs for a 6.0ml elution sample). However, values obtained from Implants 4-18 resulted in a count range of ~9500CPMs to 20CPMs, requiring the inclusion of data points in the range of <200CPMs, points that would normally not be included. Furthermore, when these values were multiplied by the appropriate factor in the extrapolative method, this created values that were high enough to affect the % ZA mass eluted. For

example, if a 1.0ml aliquot of serum were analyzed to reveal 100CPMs (below the cutoff value) the total CPMs for that 6.0ml sample would be 600CPMs – a value that would be considered significant in a range of ~9500CPMs to 20CPMs, but much less significant in a range of ~100,000CPMs to 800CPMs. The larger disparity apparent between data points and background values in Implants 1-3 (higher dose) would have prevented the inclusion of lower values and thus did not create values in excess of 100%. This problem was most prevalent in serum samples, where a smaller portion of the sample was analyzed thereby leaving room for a greater source of error due to the multiplication factors used with the extrapolation method.

It is not known what sort of elution profile is optimum for enhanced peri-implant bone formation. However, the biphasic profile characterized for HA-coated porous tantalum implants has certainly been shown to be effective in animal models. The initial burst release could be argued to be helpful for initial binding of ZA to peri-implant bone while the subsequent slower release rate could be argued to be helpful for more continuous exposure of healing bone to ZA in the longer term. The elution profile generated for implants soaked in serum is more likely to represent what occurs *in vivo*. This suggests that while there still an initial burst release, the subsequent dissolution of remaining ZA is completed relatively soon after surgery.

6.4.2 *Elution Profile from Grit Blasted Solid Titanium Implants*

Since many non-cemented joint replacement devices are not porous coated but either grit blasted or HA-coated, elution experiments were also performed for these types of surfaces. Initial release of ZA from the HA-coated grit blasted implants immersed in water (mean = 29.2%) was slightly lower than the rate of release from HA-coated porous tantalum (mean = 36.5%) in water. Values between these groups remained similar until 30 minutes when the rate of release from the grit-blasted implants surpassed the rate at which the drug eluted from the porous tantalum implants. Even though both groups of implants displayed a steady state release at 1 hour, the grit blasted implants had a greater mean amount of drug released at this time point (68.1%) as compared to tantalum implants (47.2%).

The release profile of the HA-coated grit blasted implants immersed in serum was quite similar to the profile observed for the HA-coated tantalum implants in water with a mean initial rate of release of 65.1% for the former and 68.3% for the latter within the first 5 minutes. Furthermore, at 15 minutes both groups of HA-coated implants in serum released approximately 80% of the drug and full release of the drug essentially occurred within 24 hours for both implant types.

The rate of ZA elution from HA-coated implants in serum was faster than in water, corroborating the results obtained with the porous tantalum implants. Of interest is that the biphasic release profile persisted for HA-coated grit blasted implants in both water and serum. The initial burst release may have been due to unbound ZA on the implant surface, perhaps due to saturation of HA binding sites, hydrating quickly into solution. The somewhat slower subsequent release may have been the result of partial chemical binding to the HA coating.

6.4.3 Analysis of additional samples

Analysis of the jig spindles indicated that a measurable amount of ^{14}C (0.00289 μg of ZA per spindle) had accumulated. Such an amount of drug represented about 6% of the initial starting dose, when both spindles were considered. It is therefore possible that the spindles were a source of additional ZA transfer to the implants; this would explain some of the elution readings greater than 100%.

This study demonstrated that the use of ^{14}C -labeled ZA is an effective and accurate method for characterizing the elution of ZA from HA-coated and uncoated porous tantalum and grit blasted implants. The measurement of radioactive labelled compound by liquid scintillation eliminated numerous problems and chemical complexities encountered with other measurement modalities such as mass spectroscopy, negative-ion electrospray and ultra-violet visible molecular absorption.

Figure 6.14, displays the differences in elution results obtained in the present study and in a prior study by White [66]. When UV spectroscopy was used to measure ZA elution from HA-coated porous tantalum implants in water a biphasic profile was also obtained but the rate of elution differed substantially. The liquid scintillation study presented in this thesis indicated just over half the release rate of ZA at 5 minutes (36.5%) compared with that reported using UV Spectroscopy (58.8%), with much slower subsequent elution out to 14 weeks.

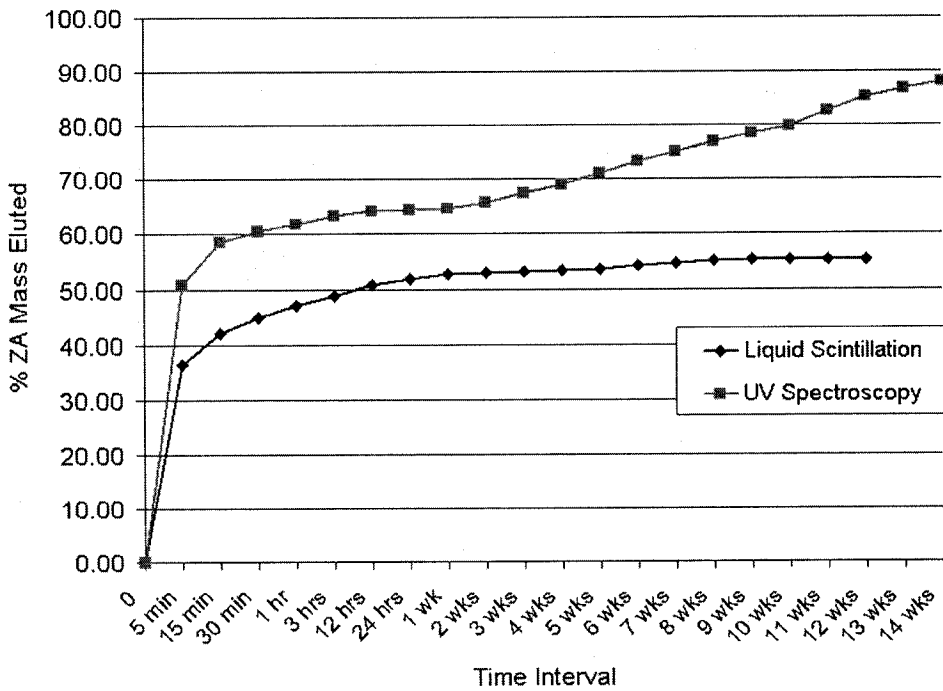


Figure 6.14 Comparison of elution techniques using either LSC or UV spectroscopy [66]. Both studies were conducted with HA coated porous tantalum metal implants immersed in water.

The elution profiles were very similar for all implants in the same groups (i.e. water or serum), indicative of the reproducibility of the technique of ZA dosing and the technique of measuring radiolabelled ZA. Elution results from non-HA coated implants indicated the rapid release of the drug, as would be expected since dehydrated compound would quickly rehydrate once in aqueous solution. It is not exactly known what sort of biologic response would occur using implants without HA coating, although the results from the rat study in Chapter 5 suggest that an initial burst release of ZA would still be effective for enhancing peri-implant bone formation. Additional analysis of local delivery of ZA from implants immersed in whole blood will be required to determine the elution profile that most resembles *in vivo* conditions. However, due to time constraints, this thesis did not explore the elution of ZA in whole blood.

7.0 DISTRIBUTION OF ¹⁴C-LABELED BISPHOSPHONATE AFTER LOCAL ELUTION FROM POROUS IMPLANTS

7.1 Purpose

ZA has been demonstrated to increase peri-implant bone formation when locally delivered from an eluting implant. Ancillary studies have also shown the release profile of ZA from a locally eluting porous tantalum implant when immobilized with HA. However, it is still unknown to what extent eluted ZA remains local to the site of implantation, only affecting the bone remodelling response in the immediate area of the implant. Localization of ZA primarily at the site of implantation would be desirable to keep the effect where it is most needed and eliminate the risk of systemic side effects. Furthermore, localization of the drug would prevent unnecessary changes to the normal remodelling cycle of healthy bone in the rest of the skeleton. Therefore, the purpose of this study was to quantify the localization and systemic distribution of ZA after elution from an implant.

7.2 Materials and Methods

7.2.1 Preparation of Tantalum Implants

Three porous tantalum implants (50mm in length and 5mm in diameter) (Trabecular Metal™, Zimmer, Warsaw IN), were plasma-sprayed coated with a thin layer (10-15µm) of HA of 98% purity, 99% density, 64% crystallinity and a calcium:phosphate ratio of 1.67. Each implant was

placed into a freely movable jig (Figure 6.4) where it was evenly and uniformly coated with a pre-prepared solution of ZA. The doping solution was prepared to contain 100µg ¹⁴C-labelled ZA (specific activity=6.51 MBq/mg) in 500µl of ddH₂O. This solution was stirred (vortexed) for one minute prior to doping to ensure even drug distribution within the vial. Using a micropipette, 100µl of the solution was applied for every 1/5 rotation of the jig. After doping, implants were placed into the oven to dry at 50°C overnight and the jig monitored with a Geiger counter to ensure contamination had not occurred. Dry implants were packaged and gas sterilized. One implant was surgically inserted within the left femoral intramedullary canal in each of three dogs in a manner similar to that described by *Tanzer et al* for ulnar implants [52].

7.2.2 Preparation of Harvested Bones for Analysis

After a time interval of 6 weeks the animals were sacrificed and the left and right femora, tibia, radius and humerus were harvested and cleaned of soft tissue. Femora containing the radioactive implant were imaged by contact radiography to display the location of the implant (Figure 7.1). Based on landmarks provided by the contact radiograph, 1-cm thick transverse serial sections were cut with a bandsaw and carefully placed into pre-labelled containers. Implants were sliced into ~1cm long sections with the bone sample where they were located in two of the canines (animals 1 and 2). The remaining dog (animal 3) had the implant removed

by bi-valving the femur to try to remove the implant intact – this resulted in implant removal in 2 pieces. Any osseous tissue adhering to the implant pieces was shaved with a scalpel and added to the appropriate container from which that implant section had been located. The implant pieces were collected and placed into a separate container for each dog.

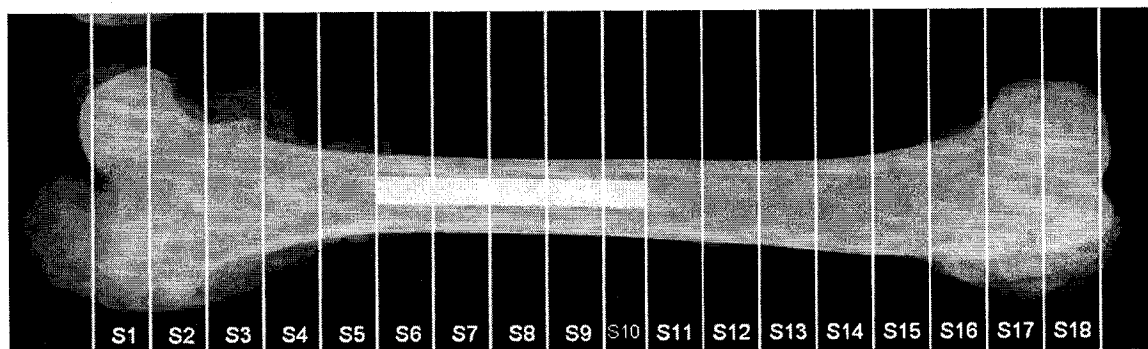


Figure 7.1 Radiograph of harvested femur containing ZA-doped implant at 6-weeks. Illustration depicts location of sections for C-14 analysis

The right femur and left and right tibia were each sliced with a bandsaw to produce three 1-cm long transverse sections from the proximal metaphysis, middle diaphysis and distal metaphysis and placed into labelled containers. The radius and humerus were sectioned in the same manner, with the exception that 0.5-cm long transverse sections were prepared.

7.2.3 De-fatting and Drying of Bone Segments

Each bone segment was placed in a container with approximately 25ml of ether-acetone (50:50) solution for a period of 24 hours. The metaphyseal sections were each drilled to create small holes to allow infiltration of the

de-fatting solution prior to immersion in ether-acetone. Following de-fatting, samples were transferred to new containers and immersed in approximately 25ml of 100% ethyl alcohol overnight to dehydrate the bones. Remaining ether-acetone and ethyl alcohol solutions were poured off and collected into two large containers and stored for later analysis. The dehydrated bone segments were transferred to an oven and dried for a period of 4 hours at 50°C.

7.2.4 Grinding and Dissolving of Bone Segments

Once dried, each bone segment was placed into a small plastic bag and mechanically pulverised with a hammer. The pulverized sample was transferred to a bone mill and ground into a fine powder (Figure 7.2). Grinding was conducted within the safe confines of a fume hood with Geiger monitoring conducted upon completion. Furthermore, this process was conducted while wearing a respirator mask to prevent inhalation of any radioactivity present in the ultra-fine bone powder released into the air when the grinder was opened. After grinding, each bone sample was transferred to a clean, pre-weighed container and the contents were weighed to determine the mass of the dried bone sample.

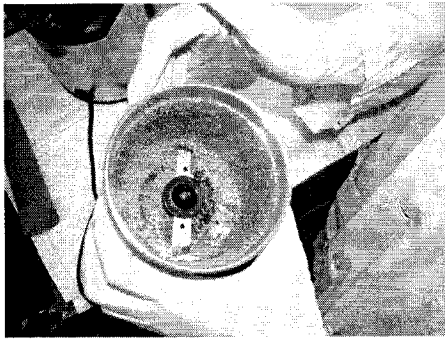


Figure 7.2 Ground bone in bone mill

The powder was immersed in 6N HCl (5ml of acid per 1g of bone) to create a bone slurry and left in an oven at 37°C for 4 days to ensure dissolution. Twice daily each container of bone solution was removed from the oven and vortexed for one-minute to aid in the dissolution. Upon dissolution the samples were cooled and then weighed to determine the mass of each bone solution.

7.2.5 Analysis of Bone Solution

Each container of bone solution was vortexed for one minute to ensure uniform distribution of the drug within the sample. A 600 μ l aliquot of liquid was removed from each sample and placed into a clean vial. To each vial 1.2ml of distilled deionized water was added and the vial was vortexed to dilute the sample to 2N HCl. Diluted samples were placed into a scintillation cocktail (Ultima Gold AB, Perkin Elmer USA) in a ratio of 10:1 of cocktail to bone solution and lightly agitated by hand. These samples were placed into a Packard Tri-Carb 2100TR liquid scintillator spectrometer (LSC) to analyze the level of ^{14}C in counts per minute (CPM) in each sample. The ZA concentration in each bone sample (ng ZA/g dry

bone) was determined after subtraction for background count using a 12-point calibration curve (Figure 6.6). As the volume and mass of the entire bone solution was known, the actual CPMs and thus the concentration in the bone sample could be extrapolated from the LSC data. Since BPs are not found to be metabolized in mammals, the radioactivities were presumed to originate from unchanged drugs [67]. Data were compared between the bone samples from the metaphysis to the samples from the diaphysis using paired student's t tests with $p=0.05$.

7.2.6 Analysis of De-fatting and Drying Solutions

After analysis of the femur and tibia from each canine it was thought that some radioactivity may have been lost to the de-fatting (ether-acetone) and drying (ethyl alcohol) solutions. Both of these solutions had been reserved and combined from all the bone samples. Therefore, 0.6ml of each of these solutions was placed into a vial containing scintillation cocktail (3:1 ratio of cocktail to solution) to mimic the amount of bone sample that was analyzed. Radius and humerus sections were analyzed at a later time, allowing the possibility to reserve the separate de-fatting and drying solutions from each bone slice. To confirm the individual sample loss of beta-radiation in the de-fatting and drying solution, both radius and humerus bones were sectioned, de-fatted and dried similarly to the bones without the implant. However, for these samples each individual de-fatting and drying solution for each bone was conserved in individual

containers – this enabled analysis of radioactivity in the fluid from each separate bone slice.

7.2.7 Analysis of Radioactivity in Harvested Implant

It was also of interest to determine the amount of radioactivity (and hence drug remaining) bound to the tantalum implant. To determine the best way to process implant pieces, two different methods of preparation were analyzed. The first method involved taking a 1cm segment of the implant from dog #1 and preparing it in the manner of the bone samples as described above, by soaking in 6N HCl for 4 days, while another 1-cm implant segment from the same dog was placed in an equivalent volume of ddH₂O for the same period of time.

When samples were analyzed by LSC, the concentration in the implant piece soaked in acid showed a 28-fold higher concentration than the one soaked in water. This led to the supposition that the implant piece soaked in ddH₂O still contained drug that was not detectable by the LSC (likely because of physical interference). To confirm this idea, the implant piece soaked in water was placed in 6N HCl for 4 days, whereupon it was re-analyzed. Based on the results of the analysis, the remaining implants were immersed in 6N HCl for 4 days and analyzed by LSC.

7.3 Results

7.3.1 Localization and Distribution of ZA in Site of Implantation and Other Bones

The mean ZA values for 1-cm intervals along the 3 test femora and 21 other bones are listed in Table 7.1. The most striking observation was that very high amounts of ZA were present within the bone samples immediately adjacent to the implants – these values ranged from 391ng to 1143 ng ZA/ g of dry bone, with a mean of 732 ng ZA/g dry bone.

Bone Section (cm)	1	2	3	4	5	6	7	8	9	10	11	12	13	14	15	16	17	18
Mean for 3 Test Femora	21	72	406	500	709	1057 	560 	1143 	510 	391 	154	37	25	16	21	19	12	8
Mean for L-Tibia, R-Femur, R-Tibia				10						2								8
Mean for R and L Humerus				12						2.5								3
Mean for R and L Radius				5.5						2								10

Table 7.1 Concentration of ZA (nanograms per g of dry bone), I=section adjacent to the implant.

As little as 1 cm proximal or distal to the implant location the values diminished markedly, by up to an order of magnitude (Figure 6.4). Excluding the 5cm region immediately adjacent to the implants, the mean ZA concentration for the 3 femora with implants was 132 ng ZA/g of bone

(range= 4 ng to 375 ng ZA/g). All bone samples contained measurable amounts of ^{14}C indicating diffusion of ZA into the circulation and a level of systemic distribution. This level was very low, however, with ZA levels in bones without the implant 1 to 3 orders of magnitude less those measured within the test femora directly exposed to ZA elution

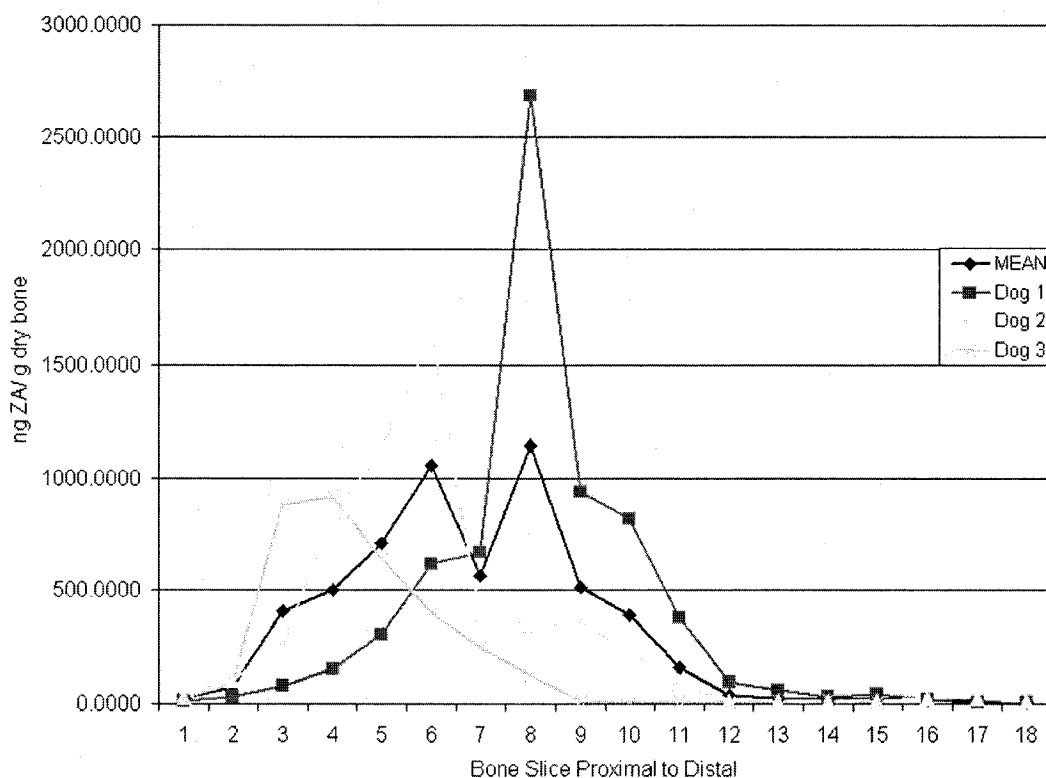


Figure 7.3 Nanograms ZA/g dry bone for each of the Left Femurs along the 18 cm bone length (at each 1 cm interval). Values are much higher immediately adjacent to the implant (slices 6-10) and fall off quickly proximal and distal to the implant.

Readings of the remaining bones showed that although drug was present, the amount was generally very low, with somewhat greater amounts present in the metaphysis than the diaphysis. Every bone sample from the metaphysis of the 21 bones without the implant (mean= 9.2 ng ZA/g

bone) contained more ZA than bone samples from the diaphysis (mean= 2.2 ng ZA/g bone), a 4-fold mean difference that was significant at $p < 0.002$ (Figure 6.5). Absolute values in these 21 bones ranged from 0.5 ng to 22.6 ng with a mean of 6.1 ng ZA/ g dry bone, about 21-fold less in magnitude than the mean concentration present in the bone samples proximal and distal to the implants and about 120-fold less in magnitude than the mean ZA concentration present in the 15 bone samples immediately adjacent to the 3 implants. Furthermore, it was observed that a higher drug concentration was present in the distal end of the radius, rather than the proximal end, in contrast to the average values observed for the other bones (Figure 6.5). However, all values observed in bones outside of the left femur containing the implant were quite low.

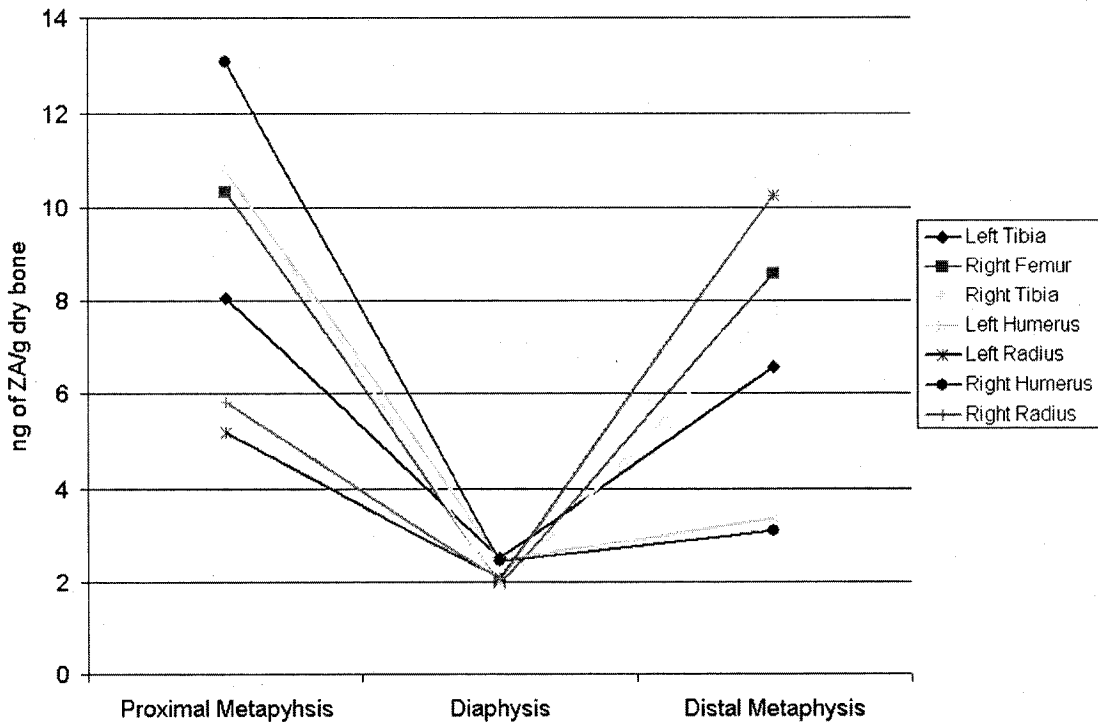


Figure 7.4 Lower concentrations of drug are always observed in the diaphysis of each bone.

7.3.2 Analysis of De-fatting and Drying Solutions

Analysis by LSC revealed only a small amount of ^{14}C in the combined de-fatting solution. This sample yielded an average of 352 CPMs, which translated $6.33 \times 10^{-4} \mu\text{g}$ of ZA. Analysis of individual de-fatting solutions from both humerus and radii revealed an average of $0.03 \mu\text{g}$ of ZA per bone sample. On average there was twice the amount of ZA observed in the solution reserved from the distal segments ($0.045 \mu\text{g}$ of ZA) than in either the proximal metaphysis ($0.021 \mu\text{g}$ of ZA) or in the diaphyseal sections ($0.027 \mu\text{g}$ of ZA). Sections analyzed from the distal radius had more ZA ($0.05 \mu\text{g}$) than in the proximal radius ($0.022 \mu\text{g}$) while the diaphysis contained only $0.013 \mu\text{g}$ of ZA on average per sample.

Unlike the ether-acetone solution, analysis of the various ethyl alcohol solutions from the different bone samples revealed counts that were equivalent to background radiation; they were therefore not considered a source of drug presence.

7.3.3 Analysis of Radioactivity in Harvested Implant

The implant soaked in acid solution had nearly the same value whether the implant was contained in the vial or whether it was removed during scintillation counting. In contrast, the implant section soaked in water showed nearly half the concentration of drug present when the implant was removed. This confirmed the thought that acid soaking was effective

for solubilizing remaining ZA and provided the rationale for soaking the remaining implant pieces in acid. Analysis of the remaining pieces showed that 19 μg to 44 μg of ZA remained bound to the different implants six-weeks after surgery (Table 7.2).

7.3.4 Total Estimate of ZA Distribution and Loss

It was determined that an average of 10.9 μg ZA was present within a canine femur containing a ZA-dosed implant, as seen in Table 7.2 in the column indicating the mass of the ZA in the femur with the implant. A similar estimate could not easily be made for the other bones (i.e. both humeri, both radii, both tibiae and the right femur) because they were only sampled at three discrete locations. Additionally, between 0.2 to 0.6 μg of ZA was recovered in the de-fatting solutions from all the bones, with an average of 0.37 μg of ZA. These values were determined by summing the amount of ZA that was recovered from each bone solution for each dog. However, when the drying solutions were similarly analyzed and the values for each solution recorded, negligible amounts of drug was observed. This means that the amount of drug lost to sample preparation and excretion or present in other parts of the skeleton varied between about 41.1% to 69.1% for the three animals.

Dog	M _{ZA} in Femur with Implant (µg)	M _{ZA} in Implant (µg)	M _{ZA} in Ether-Acetone (µg)	M _{ZA} in Alcohol (µg)	M _{ZA} - Other* (µg)
1	12.9	44.6	0.6	0.0	41.9
2	9.5	19.6	0.3	0.0	70.6
3	10.2	19.4	0.2	0.0	70.2

*Table 7.2 Total mass of ZA (M_{ZA}) accounted for in bones analyzed, implant, and defatting and drying solutions. Values for Ether-Acetone and Alcohol are the combined values of the mass of ZA in each solution. *M_{ZA} lost in sample preparation, or excreted, or present in other parts of the skeleton.*

7.4 Discussion

7.4.1 Localization and Distribution of ZA in Site of Implantation and Other Bones

The results of this study clearly demonstrated that ZA remains mostly local to the site of implantation when delivered from an eluting implant. Furthermore, systemic distribution of the drug does occur, although it is very low and well below the therapeutic dose required to elicit an effect on skeletal bone remodelling. This is supported by the observation in ancillary studies that increases in net bone formation around ZA-dosed porous tantalum implants are very much confined to the immediate peri-implant space [52], where the ZA concentration was measured in this study to be at least two orders of magnitude greater than in remote sites of the skeleton.

It is presumed that systemic delivery results from diffusion of the drug from the implant site into the circulation. It was observed that a greater amount of ZA was observed in the metaphyseal sections compared with the

diaphysis. This is probably due to the higher surface area of this bone and the higher prevailing rate of bone turnover in cancellous bone.

As table 7.2 demonstrates, between 30-60% of the starting dose was recovered in osseous tissues, the implant and defatting solutions, leaving about 40-70% of the starting dose presumably present in other parts of the skeleton that weren't analyzed or lost through excretion. Given the very small amounts that were measured in the bones that were analyzed, it is reasonable to think that a considerable amount of ZA was excreted. The *in vitro* elution studies in serum described in Chapter 6 indicated that 68% of the drug was released within the first 5 minutes, with complete elution occurring by one week. An undetermined portion of this apparently would diffuse into the bloodstream; this would result in an immediate loss of 30-80% through urinary excretion, as described by *Ezra et al* [47]. Excretion in fecal matter is expected to be quite low, as *Lin et al* found that only 0.36% of a dose of ^{14}C -alendronate was recovered in fecal matter after 24 hours [50].

The residual amount of ZA measured on the implants after 6 weeks is in conflict with the elution data in serum that showed complete elution of ZA within 1 week (Chapter 6). This discrepancy is hypothesized to be related to the use of EDTA in the serum elution studies of Chapter 6 causing the rapid release of the drug. Additionally, the high readings of radioactivity

observed on the implant pieces may have been due to the presence of retained bone within the implant. Although it was attempted to remove bone from the implants, it was not possible to remove bone that formed within the internal struts of the trabecular structure. As such, it is postulated that readings of radioactive ZA were at least partially the result of drug bound to the bone attached to the inner struts, rather than to the metallic implant itself. The elution data in serum (Chapter 6) would need to be repeated without EDTA to see how they correspond with the measurements of ZA on/within the implant pieces."

It was observed that Dog 1 greatly differed in the amount of drug remaining bound to the implant, with just over double the amount remaining, as compared to the other animals. It is unknown why such a large variation existed between this animal, while the other two canines had nearly equivalent results. Even though the amount of ZA drug remaining on the implant in Dog 1 was much greater than in Dogs 2 and 3, the other ZA values recorded in the bone sections and ether-acetone solution were all similar. Further research will be required with a larger group of animals to determine the expected residual amount of drug on the implant to determine whether the outlier in this group is due to measurement error or to natural variance between animals.

Small but measurable amounts of ZA were observed in the collected ether-acetone solutions. Since ether-acetone solution was used to remove fat from the bone segments, the presence of ZA in these solutions indicated the presence of ZA in the fatty substance of the bone marrow. The ether-acetone was effective in removing residual ZA in the bone segments given that only background counts were measured in the ethyl alcohol solution, as indicated in Table 7.2.

Further work will be necessary to track the amount of drug lost through all routes (e.g. waste products) as well as localization in other bones and soft tissues. However, as demonstrated by this single low dose study, ZA has a high affinity for bone, thus little drug would be expected to be located in the soft tissues and organs. It would be helpful to conduct longer term studies of this type to ascertain the skeletal distribution of ZA over time. Autoradiography could also be conducted to quantify the ZA concentration and location in the peri-implant bone throughout the bone sections. The extremely low levels of ZA that existed remote from the implant would probably mitigate against any risk of complications from ZA exposure, an added advantage of local elution directly from an implant.

8.0 CONCLUSION

As inhibitors of bone resorption bisphosphonates have potential use for enhancing peri-implant bone formation. This has been demonstrated in several independent studies using both systemic and local delivery of the compound, most often with ZA, a potent third generation bisphosphonate. It would appear that local delivery of ZA to the implant site is an ideal approach since it targets the area of interest and avoids or minimizes skeletal exposure.

This thesis has provided insight into several aspects of the concept of using ZA in conjunction with orthopaedic implants. A simple and inexpensive rat model was described that enables the use of microCT for quantifying the local bone response around an implant. An accurate method was developed for characterizing the elution profiles of ZA from different implant types of implants using radiolabelled compound. Finally, the extent to which locally eluted ZA remains at the implant site and is skeletally distributed was ascertained in a 6 week canine model. Based on the results of these experiments suggestions were made for further studies that will add to the knowledge base of the concept of local bisphosphonate elution from orthopaedic devices.

9.0 REFERENCES

1. Radin, E.L., Who Gets Osteoarthritis and Why?, *The Journal of Rheumatology* (2004) 31: 10-15
2. Bobyn, J.D., Toh, K.K., Hacking, S.A., Tanzer, M., Krygier, J.J., Tissue response to porous tantalum acetabular cups: a canine model, *J. Arthroplasty* (1999) 14: 347-354
3. Moore, A.T., Metal hip joint: a new self-locking vitallium prosthesis, *South Med. J.* (1952) 45: 1015-1019
4. Kienapfel, H., Sprey, C., Wilke, A., Griss, P., Implant Fixation by Bone Ingrowth, *The Journal of Arthroplasty* (1999) 14: 355-368
5. Galante, J., Rostoker, W., Lueck, R., Ray, R.D., Sintered Fiber Metal Composites as a Basis for Attachment of Implants to Bone, *J. Bone Joint Surg. Am.* (1971) 53: 101-114
6. Hirschhorn, J.S., McBeath, A.A., Dustoor, M.R., Porous Titanium Surgical Implant Materials, *J. Biomed. Mater. Res. Symp. II* (1971) 2: 49-67
7. Hahn, H., Palich, W., Preliminary evaluation of Porous Metal Surfaced Titanium for Orthopaedic Implants, *J. Biomed. Mater. Res.* (1970) 4: 571-577
8. Cameron, H.U., Pilliar, R.M., MacNab, I., The Effect of Movement on the Bonding of Porous Metal to Bone, *Clin. Orthop.* (1973) 7: 301-311
9. Bobyn, J.D., Pilliar, R.M., Cameron, H.U., Weatherly, G.C., Osteogenic Phenomena Across Endosteal Bone-Implant Spaces with Porous Surfaced Intramedullary Implants, *Acta. Orthop. Scand.* (1981) 52: 145-153
10. Dalton, J.E., Cook, S. D., Thomas, K.A., Kay, J.F., The effect of operative fit and hydroxyapatite coating on the mechanical and biological response to porous implants, *J. Bone Joint Surg. (Am)* (1995) 77: 97-110
11. Bobyn, J.D., Pilliar, R.M., Cameron, H.U., Weatherly, G.C., The Optimum Pore size for the fixation of porous surfaced metal implants by the ingrowth of bone, *Clin. Orthop. Relat. Res.* (1980) 150: 263-270
12. Hacking, S.A., Harvey, E.J., Tanzer, M., Krygier, J.J., Bobyn, J.D., Acid-etched microtexture for enhancement of bone ingrowth into

- porous coated implants, *The Journal of Bone and Joint Surgery (Br)* (2003)85-B: 1182-1189
13. Bobyn, J.D., Stackpool, G.J., Hacking, S.A., Tanzer, M., Krygier, J.J., Characteristics of bone ingrowth and interface mechanics of a new porous tantalum material, *J. Bone Joint Surg. (Br)* (1999) 81B: 907-914
 14. Lind, M., Bunger, C., Factors stimulating bone formation, *Eur Spine J* (2001) 10: S102-S109
 15. Kienapfel, H., Sumner, D.R., Turner, T.M., Urban, R.M., Galante, J.O., Efficacy of Autograft and Freeze-Dried Allograft to Enhance Fixation of Porous Coated Implants in the Presence of Interface Gaps, *J. Orthop. Res.* (1992) 10: 423-433
 16. Tagil, M., The morselized and impacted bone graft. Animal experiments on proteins, impaction and load., *Acta Orthop Scand Suppl.* (2000) 290: 1-40
 17. Pietrzak, W., Perns, S., Keyes, J., Woodell-May, J., McDonald, N., Demineralized Bone Matrix Graft: A Scientific and Clinical Case Study Assessment, *The Journal of Foot and Ankle Surgery* (2005) 44: 345-353
 18. Sudo, A., Hasegawa, M., Fukuda, A., Kawamura, G., Muraki, M., Uchida, A., Acetabular Reconstruction Using a Cementless Cup and Hydroxyapatite Granules 3 to 8 Year Clinical Results, *J. Arthroplasty* (2007) 22: 828-832
 19. Aufdemorte, T.B., Fox, W.C., Holt, R.H., McGuff, H.S., Ammann, A.J., Beck, L.S., An Intraosseous Device for Studies of Bone-Healing, *JBJS (Am)* (1992) 74: 1153-1161
 20. Wozney, J.M., Rosen, V., Celeste, A.J., Mitsock, L.M., Whitters, M.J., Kriz, R.W., Hewick, R.M., Wang, E.A., Novel Regulators of Bone Formation: Molecular Clones and Activities, *Science* (1988) 242: 1528-1534
 21. Kang, P., Shen, B., Yang, J., Cheng, J., Pei, F., Repairing Defect and Preventing Collapse of Canine Femoral Head Using Titanium Implant Enhanced Autogenous Bone Graft and rhBMP-2, *Connective Tissue Research* (2007) 48: 171-179
 22. Mundy, G. R., Pathogenesis of osteoporosis and challenges for drug delivery, *Advanced Drug Delivery Reviews* (2000) 42: 165-173

23. Tanzer, M., Kantor, S., Bobyn, J.D., Enhancement of bone growth into porous intramedullary implants using non-invasive low intensity ultrasound, *Journal of Orthopaedic Research* (2001)19: 195-199
24. Geesink, R., Osteoconductive Coatings for Total Joint Arthroplasty, *Clinical Orthopaedics and Related Research* (2002) 395: 53-65
25. Oonishi, H., Orthopaedic Applications of Hydroxyapatite, *Biomaterials* (1991) 12: 171- 178
26. Hacking, S.A., Tanzer, M., Harvey, E.J., Krygier, J.J., Bobyn, J.D., Relative Contributions of Chemistry and Topography to the Osseointegration of Hydroxyapatite Coatings, *Clinical Orthopaedics and Related Research* (2002) 405: 24-38
27. Tanzer, M., Gollish, J., Leighton, R., Orrell, K., Giacchino, A., Welsh, P., Shea, B., Wells, G., The Effect of Adjuvant Calcium Phosphate Coating on a Phosphate Coating on a Porous-Coated Femoral Stem, *Clinical Orthopaedics and Related Research* (2004) 424: 153-160
28. Zardiackas, L.D., Parsell, D.E., Dillon, L.D., Mitchell, D.W., Nunnery, L.A., Poggie, R., Structure, metallurgy and mechanical properties of a porous tantalum foam, *J. Biomed. Mater. Res. (Appl. Biomater)* (2001) 58: 180-187
29. Ryan, G., Pandit, A., Apatsidis, D.P., Fabrication methods of porous metals for use in orthopaedic applications, *Biomaterials* (2006) 27: 2651-2670
30. Ganguli, A., Henderson, C., Grant, M.H., Meikle, S.T., Lloyd, A.W., Goldie, I., The interactions of bisphosphonates in solution and as coatings on hydroxyapatite with osteoblasts, *Journal of Material Science: Materials in Medicine* (2002) 13: 923-931
31. Russell, R.G.G., Rogers, M.J., Bisphosphonates: From the Laboratory to the Clinic and Back Again, *Bone* (1999) 25: 97-106
32. Martin, T.J., Grill, V., Bisphosphonates-Mechanisms of action, *Austr. Prescr.* (2000) 23: 130-132 & DeRuiter, J., Clark, R., Bisphosphonates: Calcium Anti-resorptive Agents, *Endocrine Module* (Spring 2002)
33. Russell, R.G.G., Bisphosphonates: Mode of Action and Pharmacology, *Paediatrics* (2007) 119: 2: S150-S162

34. Zou, X., Xue, Q., Li, H., Bunger, M., Lind, M., Bunger, C., Effect of alendronate on bone ingrowth into porous tantalum and carbon fiber interbody devices, *Acta Orthopaedica Scandinavica* (2003) 74: 596 – 603
35. Goto, T., Kajiwara, H., Yoshinari, M., Fukuhara, E., Kobayashi, S., Tanaka, T., In vitro assay of mineralized-tissue formation on titanium using fluorescent staining with calcein blue, *Biomaterials* (2003) 22: 3885-3892
36. Bauss, F., Lalla, S., Endelle, R., Hothorn, L.A., Effects of treatment with Ibandronate on Bone Mass Architecture, Biomechanical Properties, and Bone Concentration of Ibandronate in Ovariectomized monkeys, *The Journal of Rheumatology* (2002) 29: 2200-2208
37. Black, D.M., Delmas, P.D., Eastell, R., Reid, I.R., Boonen, S., Cauley, J.A., Cosman, F., Lakatos, P., Leung, P.C., Man, Z., Mautalen, C., Mesenbrink, P., Hu, H., Caminis, J., Tong, K., Rosario-Jansen, T., Krasnow, J., Hue, T.F., Sellmeyer, D., Eriksen, E.F., Cummings, S.R., Once Yearly Zoledronic Acid for Treatment of Postmenopausal Osteoporosis, *New England Journal of Medicine* (2007) 356: 1809-1822
38. Lyles, K.W., Colon-Emeric, C.S., Magaziner, J.S., Adachi, J.D., Pieper, C.F., Mautalen, C., Hyldstrup, L., Recknor, C., Nordsletten, L., Moore, K.A., Lavecchia, C., Zhang, J., Mesenbrink, P., Hodgson, P.K., Abrams, K., Orloff, J.J., Horowitz, Z., Eriksen, E.F., Boonen, S., Zoledronic Acid and Clinical Fractures and Mortality after Hip Fracture, *New England Journal of Medicine* (2007) 357: 1799-1809
39. Higano, C., Annual Zoledronic Acid: Is Less More?, *Journal of Clinical Oncology* (2007) 25: 1026
40. Little, D.G., Peat, R.A., McEvoy, A., Williams, P.R., Smith, E.J., Baldock, P.A., Zoledronic Acid Treatment Results in Retention of Femoral Head Structure After Traumatic Osteonecrosis in young Wister Rats, *Journal of Bone and Mineral Research* (2003) 18: 2016-2022
41. Little, D.G., McDonald, M., Sharpe, I.T., Peat, R., Williams, P., McEvoy, T., Zoledronic Acid improves femoral head sphericity in a rat model in perthes disease, *Journal of Orthopaedic Research* (2005) 23: 862-868

42. Bobyn, J.D., Hacking, S.A., Krygier, J.J., Harvey, E.J., Little, D.G., Tanzer, M., Zoledronic Acid causes enhancement of bone growth into porous implants, *J. Bone Joint Surg. (Br)* (2005) 87B: 416-420
43. Tagil, M., Aspenberg, P., Astrand, J., Systemic zoledronate precoating of a bone graft reduces bone resorption during remodeling, *Acta Orthopaedica* (2006) 77: 23-26
44. Pampu, A.A., Dolanmaz, D., Tuz, H.H., Karabacakoglu, A., Experimental Evaluation of the Effects of Zoledronic Acid on Regenerate Bone Formation and Osteoporosis in Mandibular Distraction Osteogenesis, *J Oral Maxillofac. Surg.* (2006) 64: 1232-1236
45. Bransford, R., Goergens, E., Briody, J., Amanat, N., Cree, A., Little, D., Effect of Zoledronic Acid in an L6-L7 rabbit spine fusion model, *Eur. Spine J.* (2007) 16: 557-562
46. Matos, M.A., Araujo, F.P., Paixao, F. B., The effect of zoledronate on bone remodelling during the healing process, *Acta Ciurgica Brasileira* (2007) 22: 115-119
47. Ezra, A., Goloumb, G., Administration routes and delivery systems of bisphosphonates for the treatment of bone resorption, *Adv. Drug. Deliv. Rev.* (2000) 42: 175-195
48. DeRuiter, J., Clark, R., Bisphosphonates: Calcium Anti-resorptive Agents, *Endocrine Module* (Spring 2002)
49. Gertz, B.J., Holland, S.D., Kline, W.F., Matuszewski, B.K., Porras, A.G., Clinical Pharmacology of Alendronate Sodium, *Osteoporosis International* (1993) Suppl. 3: S13-S16
50. Lin, J.H., Bisphosphonates: A Review of Their Pharmacokinetic Properties, *Bone* (1996) 18: 75-85
51. Legay, F., Gauron, S., Deckert, F., Gosset, G., Pfaar, U., Ravera, C., Wiegand, H., Schran, H., Development and Validation of a Highly Sensitive RIA for zoledronic acid, a new potent heterocyclic bisphosphonate in human serum, plasma and urine, *Journal of Pharmaceutical and Biomedical Analysis* (2002) 30: 897-911
52. Tanzer, M., Karabasz, D., Krygier, J.J., Cohen, R., Bobyn, J.D., Bone Augmentation around and within Porous Implants by Local Bisphosphonate Elution, *Clinical Orthopaedics and Related Research* (2005) 441: 30-39

53. Peter, B., Pioletti, D.P., Laib, S., Bujoli, B., Pilet, P., Janvier, P., Guicheux, J., Zambelli, P.-Y., J.-M., Bouler, Gauthier, O., Calcium Phosphate Drug Delivery System: Influence of Local Zoledronate Release on Bone Implant Osteointegration, *Bone* (2005) 36: 52-60
54. Kumar, D., Kumar, V. Little, D.G., Hownam-Giles, R.B., Wong, E., Ali, S.O., Evaluation of biodistribution by local versus systemic administration of ^{99m}Tc-labeled pamidronate, *Journal of Orthopaedic Science* (2006) 11: 512-520
55. Skoglund, B., Holmertz, J., Aspenberg, P., Systemic and local ibandronate enhance screw fixation, *Journal of Orthopaedic Research*(2004) 22: 1108-1113
56. Astrand, J., Aspenberg, P., Systemic alendronate prevents resorption of necrotic bone during revascularization. A bone chamber study in rats., *BMC Musculoskeletal Disorders* (2002) 3: 19
57. Astrand, J., Aspenberg, P., Topical, single dose bisphosphonate treatment reduced bone resorption in a rat model for prosthetic loosening, *J. Orthop. Res.* (2004) 22: 244-249
58. Monkkonen, J., Hanna-Maija-Maija, K., Ylitalo, P., Comparison of the Distribution of three bisphosphonates in mice, *Pharmacology & Toxicology* (1989) 65: 294-298
59. Monkkonen, J., Ylitalo, P., Elo, H.A., Airaksinen, M.M., Distribution of ¹⁴C-Clodronate (dichloromethylene BP) disodium in mice, *Toxicol. Appl. Pharmacol.* (1987) 89: 287-292
60. Smith, S.Y., Recker, R.R., Hannan, M., Muller, R., Bauss, F., Intermittent intravenous administration of the bisphosphonate ibandronate prevents bone loss and maintains bone strength, *Bone* (2003) 32: 45-55
61. Bauss, F., Lalla, S., Endelle, R., Hothorn, L.A., Effects of treatment with Ibandronate on Bone Mass Architecture, Biomechanical Properties, and Bone Concentration of Ibandronate in Ovariectomized monkeys, *The Journal of Rheumatology* (2002) 29: 2200-2208
62. Osterman, T., Virtamo, T., Kippo, K., Lauren, L., Pasanen, I., Hannuniemi, R., Sellman, R., Distribution of Clodronate in the Bone of Adult Rats and its Effects on Trabecular and Cortical Bone, *Journal of Pharmacology and Experimental Therapeutics* (1997) 280: 1051-1056

63. Peter, B., Orthopaedic Implants used as a Drug Delivery Systems: Numerical, In vitro, and In vivo studies, PhD Thesis, École Polytechnique Fédérale De Lausanne, Thèse No 3044 (2004)
64. Amanat, N., McDonald. M., Godfrey, C., Bilston, L, Little, D., Optimal Timing of a Single Dose of Zoledronic Acid to Increase Strength in Rat Fracture Repair, *Journal of Bone and Mineral Research* (2007) 22: 867-876
65. Hacking, S.A., Zuraw, M., Harvey, E.J., Tanzer, M., Krygier, J.J., Bobyn, J.D., A physical vapor deposition method for controlled evaluation of biological response to biomaterial chemistry and topography, *J. Biomed. Mater. Res. A.* (2007) 82: 179 – 187
66. White, C., 2005, Characteristics of Bisphosphonate Elution from Orthopaedic Implants [Masters thesis], Montreal, McGill University, 136pp
67. Kim, H.K.W., Sanders, M., Athavale, S., Bian, H., Bauss, F., Local bioavailability and distribution of systemically (parenterally) administered ibandronate in the infarcted femoral head, *Bone* (2006)

Animal protocols were approved by the MUHC animal care committee and conducted according to guidelines.